Zoosyst. Evol. 101 (3) 2025, 1023–1055 | DOI 10.3897/zse.101.144375

PENSOFT

MUSEUM FÜR NATURKUNDE BERLIN

Four new tube-nosed bat species of the genus *Murina* (Chiroptera, Vespertilionidae) from Xizang Autonomous Region, China, based on morphological and molecular data

Tao Luo[1,2,3*], Ming-Le Mao[2*], Chang-Ting Lan[4], Zi-Fa Zhao[2], Zhong-Lian Wang[4], Jing Yu[4], Jia-Jia Wang[2], Chen-Rui Yan[4], Ning Xiao[5], Jiang Zhou[2]

1 *School of Life Sciences, Yunnan University, Kunming, China*
2 *School of Karst Science, Guizhou Normal University, Guiyang, China*
3 *Southwest United Graduate School, Kunming, China*
4 *School of Life Sciences, Guizhou Normal University, Guiyang, China*
5 *Guiyang Healthcare Vocational University, Guiyang, China*

https://zoobank.org/798F3D1F-E08C-49AA-8662-30CBC75BF53F

Corresponding author: Jiang Zhou (zhoujiang@ioz.ac.cn)

Academic editor: Melissa TR Hawkins ♦ **Received** 13 December 2024 ♦ **Accepted** 11 April 2025 ♦ **Published** 2 June 2025

Abstract

The genus *Murina* Gray, 1842, recently had four new species discovered in China over the last four years, suggesting its diversity may have been previously underestimated. Herein, we describe four new species—*Murina beibengensis* **sp. nov.**, *Murina medogensis* **sp. nov.**, *Murina milinensis* **sp. nov.**, and *Murina yadongensis* **sp. nov.**—based on morphological and genetic evidence from specimens collected during bat diversity surveys conducted in the Xizang Autonomous Region of China over the past three years. Each of these four new species forms an independent lineage on a phylogenetic tree reconstructed using the mitochondrial COI and Cyt *b* genes, and each is genetically distinct from its congeners. Morphologically, the new species can be distinguished from the 43 recognized congeners by features including forearm length, hair color, and skull morphology. We elevated *M. huttoni rubella* from a subspecies of *M. huttoni* to a species based on morphological and genetic evidence. The new species discussed herein increase the number of species in the genus *Murina* to four worldwide and from 23 to 28 in China. This study not only enriches our understanding of bat species diversity but also underscores the importance of conducting bat surveys in the specialized highland habitats of the Himalayas.

Key Words

Diversity, Himalaya, morphology, *Murina*, taxonomy

Introduction

The family Vespertilionidae has an extremely high species diversity with over 500 species distributed worldwide (Moratelli et al. 2019). Within this family, species of the subfamily Murininae share a single prominent characteristic, namely, tube-shaped nostrils. There are three recognized genera in this subfamily: *Murina* Gray, 1842; *Harpiocephalus* Gray, 1842; and *Harpiola* Thomas, 1915 (Kuo et al. 2006; Son et al. 2015; Moratelli et al. 2019; Mou et al. 2024). For a long time, although these genera have distinguishable morphological characteristics, their phylogenetic relationships have been controversial (Tate 1941; Bhattacharyya 2002; Wilson

* These authors contributed equally to this paper.

and Reeder 2005; Kuo et al. 2006). For example, phylogenetic analyses based on the mitochondrial cytochrome c oxidase subunit I (COI) gene revealed that *Harpiocephalus* and *Harpiola* are phylogenetically embedded within *Murina* (Ruedi et al. 2012; Soisook 2013; Son et al. 2015; Tu et al. 2015; Soisook et al. 2017; Mou et al. 2024; Mou et al. 2025). However, recent phylogenomic studies have provided robust support for the taxonomic validity of these genera, recovering *Murina* as the sister clade to *Harpiocephalus* and *Harpiola*, with the phylogenetic conflicts among genera being attributable to ancient introgression events (Wang et al. 2024b).

Asian tube-nosed bats, genus *Murina* Gray, 1842, are small bats with a forearm length of less than 44 mm. These bats are largely distributed in the forests of East, South, and Southeast Asia, as well as in parts of North Asia (Moratelli et al. 2019) (Fig. 1). Based on the relative size of the crown area of the canines and first and second upper premolars, as well as the position of the incisors, the genus *Murina* has been divided into two groups (Corbet and Hill 1992). In the *suilla* group, the first upper incisor (I^2) is situated anterior to the second (I^3), I^2 is clearly visible in the lateral view, and the crown area of the first upper premolar (P^2) is half or less that of the second (P^4); meanwhile, in the *cyclotis* group, I^3 is adjacent to I^2, such that I^2 is essentially obscured by I^3 when viewed laterally, and the crown area of P^2 is 2/3 or more that of P^3 (Csorba and Bates 2005). However, these two morphogroups do not represent monophyletic groups and were therefore later revised as "*suilla*-type" and "*cyclotis*-type" (Son et al. 2015; Soisook et al. 2017; Yu et al. 2020; Mou et al. 2024; Wang et al. 2024a; Mou et al. 2025). Currently, 43 species of the genus *Murina* have been recognized (Dobson 1872; Peters 1872; Scully 1881; Thomas 1891; Sowerby 1922; Hill 1964; Hill and Francis 1984; Maeda and Matsumura 1998; Csorba and Bates 2005; Kruskop and Eger 2008; Furey et al. 2009; Kuo et al. 2009; Csorba et al. 2011; Eger and Lim 2011; Francis and Eger 2012; Soisook et al. 2013a; Soisook et al. 2013b; He et al. 2015; Son et al. 2015; Chen et al. 2017; Soisook et al. 2017; Zeng et al. 2018; Moratelli et al. 2019; Yu et al. 2020; Mou et al. 2024; Mou et al. 2025) (Table 1), with 24 species occurring in China (Mou et al. 2025; Wei et al. 2025), several of which have been discovered in the last 10 years, i.e., *M. fanjingshanensis* He, Xiao & Zhou, 2015 (He et al. 2015), *M. rongjiangensis* Chen, Liu, Deng, Xiao & Zhou, 2017 (Chen et al. 2017), *M. liboensis* Zeng, Chen, Deng, Xiao & Zhou, 2018 (Zeng et al. 2018), *M. jinchui* Yu, Csorba & Wu, 2020 (Yu et al. 2020), *M. yuanyang* Mou, Qian, Li, Li, Luo & Li, 2024 (Mou et al. 2024), *M. yushuensis* Han, Csorba & Wu, 2024 (Wang et al. 2024a), and *M. lvchun* Mou & Li, 2025 (Mou et al. 2025). These findings show that the species diversity of the genus may have been seriously underestimated.

Several new bat specimens were collected during biodiversity surveys conducted between July 2023 and August 2024 in China's Xizang Autonomous Region and Gansu Province. These specimens were identified as belonging to the genus *Murina* based on the following diagnostic characteristics: tube-shaped nose, forearm length less than 44 mm (vs. usually greater than 44 mm in *Harpiocephalus*), third upper molars (M^3) are reduced, with parastyle, paracone, and protocone (vs. highly reduced in *Harpiocephalus*, only parastyle), heights of the inner (I^2) and outer (I^3) upper incisors each measuring half the height of the upper canines (C^1) (vs. 2/3 in *Harpiola*), and the height and crown area of the first premolar (P_2) are significantly smaller than those of the lower canine (C_1) (vs. similar in *Harpiola*) (Kuo et al. 2006; Mou et al. 2024). Subsequent detailed morphological comparisons and molecular analyses indicated that these specimens could be distinguished from currently recognized species. Based on these differences, we formally describe the specimens as four new species of the genus *Murina*: *Murina beibengensis* sp. nov., *Murina medogensis* sp. nov., *Murina milinensis* sp. nov., and *Murina yadongensis* sp. nov.

Materials and methods

Taxon sampling and morphological analyses

A total of 55 specimens from the genus *Murina* were collected between July 2016 and August 2024 in a bat survey that included areas in China's Xizang, Xinjiang, Qinghai, Gansu, Guizhou, Sichuan, and Shaanxi Provinces. The experimental animals used in this study were treated in accordance with Chinese animal welfare laws (GB/T 35892–2018). All specimens used for morphological studies were fixed in 95% ethanol and stored at the Animal Ecology Laboratory of Guizhou Normal University in the city of Guiyang, Guizhou Province, China. All molecular samples were stored in a refrigerator kept at –80 °C.

Morphometric data were collected from 25 well-preserved specimens of the genus *Murina* (Suppl. material 2). A total of 25 measurements were recorded to the nearest 0.1 mm using digital calipers following the protocol of Wang et al. (2024a). For external measurements of the body, including **HB** = head-body length (from tip of snout to anus); **TL** = tail length (from anus to tip of tail); **EL** = ear length (from lower edge of external auditory meatus to tip of pinna); **EW** = ear width (maximum width of the external auditory meatus); **TRL** = tragus length (from base to tip of tragus); **TRW** = tragus width (maximum width of the tragus); **HFL** = hind foot length (from extremity of heel to tip of longest toe, not including claws); **FL** = forearm length (from elbow to carpus with wings folded); **TIB** = tibia length (from knee joint to ankle). Measurements of the cranial and dental from extracted and cleaned skull including: **GTL** = greatest length of skull (from anterior aspect of I^2 to most prominent point of occipital region); **CCL** = condylocanine length (from exoccipital condyle to most anterior part of C^1); **BCW** = braincase width (greatest width of braincase); **BCH** = braincase height (from horizontal plane to highest point

Table 1. Species catalogue, dentition types, molecular markers, and references for the genus *Murina* (modified from Moratelli et al. 2019).

ID	Species	Dentition	Molecular data	Literature obtained
1	*Murina aenea* Hill, 1964	*Cyclotis*-type	Present	Hill 1964; Moratelli et al. 2019
2	*Murina annamitica* Francis & Eger, 2012	*Cyclotis*-type	Present	Francis and Eger 2012
3	*Murina cyclotis* Dobson, 1872	*Cyclotis*-type	Present	Dobson 1872; Moratelli et al. 2019
4	*Murina fionae* Francis & Eger, 2012	*Cyclotis*-type	Present	Francis and Eger 2012
5	*Murina guilleni* Soisoo, Karapan, Satasook, Thong, Khan, Maryanto, Csorba, Furey, Aul & Bates, 2013	*Cyclotis*-type	Present	Soisook et al. 2013a
6	*Murina harrisoni* Csorba & Bates, 2005	*Cyclotis*-type	Present	Csorba and Bates 2005
7	*Murina huttoni* (Peters, 1872)	*Cyclotis*-type	Present	Peters 1872; Moratelli et al. 2019
8	*Murina lvchun* Mou & Song Li, 2025	*Cyclotis*-type	Present	Mou et al. 2025
9	*Murina peninsularis* Hill, 1964	*Cyclotis*-type	Present	Hill 1964; Moratelli et al. 2019
10	*Murina pluvialis* Ruedi, Biswas & Csorba, 2012	*Cyclotis*-type	Present	Ruedi et al. 2012
11	*Murina puta* Kishida, 1924	*Cyclotis*-type	Present	Moratelli et al. 2019
12	*Murina recondita* Kuo, Fang, Csorba & Lee, 2009	*Cyclotis*-type	Present	Kuo et al. 2009
13	*Murina rozendaali* Hill & Francis, 1984	*Cyclotis*-type	Present	Hill and Francis 1984; Moratelli et al. 2019
14	*Murina bicolor* Kuo, Fang, Csorba & Lee, 2009	*Suilla*-type	Present	Kuo et al. 2009
15	*Murina aurata* Milne-Edwards, 1872	*Suilla*-type	Present	Moratelli et al. 2019
16	*Murina balaensis* Soisook, Karapan, Satasook & Bates, 2013	*Suilla*-type	Present	Soisook et al. 2013b
17	*Murina beelzebub* Son, Furey, Csorba & 2011	*Suilla*-type	Absent	Csorba et al. 2011
18	*Murina chrysochaetes* Eger & Lim, 2011	*Suilla*-type	Present	Eger and Lim 2011
19	*Murina eleryi* Furey, Thong, Bates, Csorba & Son, 2009	*Suilla*-type	Present	Furey et al. 2009
20	*Murina fanjingshanensis* He, Xiao & Zhou, 2015	*Suilla*-type	Present	He et al. 2015
21	*Murina feae* (Thomas, 1891)	*Suilla*-type	Present	Thomas 1891; Moratelli et al. 2019
22	*Murina florium* Thomas, 1908	?	Present	Moratelli et al. 2019
23	*Murina fusca* Sowerby, 1922	*Suilla*-type	Absent	Sowerby 1922
24	*Murina gracilis* Kuo, Fang, Csorba & Lee, 2009	*Suilla*-type	Present	Kuo et al. 2009
25	*Murina harpioloides* Kruskop & Eger, 2008	*Suilla*-type	Present	Kruskop and Eger 2008
26	*Murina hilgendorfi* Peters, 1880	*Suilla*-type	Present	Moratelli et al. 2019
27	*Murina hkakaboraziensis* Soisook, Thaw, Kyaw, Oo, Pimsai, Suarez-Rubio & Renner, 2017	*Suilla*-type	Present	Soisook et al. 2017
28	*Murina jaintiana* Ruedi, Biswas & Csorba, 2012	*Suilla*-type	Present	Ruedi et al. 2012
29	*Murina jinchui* Yu, Csorba & Wu, 2020	*Suilla*-type	Present	Yu et al. 2020
30	*Murina kontumensis* Son, Csorba, Tu & Motokawa, 2015	*Suilla*-type	Present	Son et al. 2015
31	*Murina leucogaster* Milne-Edwards, 1872	*Suilla*-type	Present	Moratelli et al. 2019
32	*Murina liboensis* Zeng, Chen, Deng, Xiao & Zhou, 2018	*Suilla*-type	Present	Zeng et al. 2018
33	*Murina lorelieae* Eger & Lim, 2011	*Suilla*-type	Present	Eger and Lim 2011
34	*Murina rongjiangensis* Chen, Liu, Deng, Xiao & Zhou, 2017	*Suilla*-type	Present	Chen et al. 2017
35	*Murina ryukyuana* Maeda & Matsumura, 1998	*Suilla*-type	Absent	Maeda and Matsumura 1998
36	*Murina shuipuensis* Eger & Lim, 2011	*Suilla*-type	Present	Eger and Lim 2011
37	*Murina suilla* Temminck, 1840	*Suilla*-type	Present	Moratelli et al. 2019
38	*Murina tenebrosa* Yoshiyuki, 1970	*Suilla*-type	Absent	Moratelli et al. 2019
39	*Murina tubinaris* (Scully, 1881)	*Suilla*-type	Present	Scully 1881; Moratelli et al. 2019
40	*Murina ussuriensis* Ognev, 1913	*Suilla*-type	Present	Moratelli et al. 2019
41	*Murina walstoni* Furey, Csorba & Son, 2011	*Suilla*-type	Present	Csorba et al. 2011
42	*Murina yuanyang* Mou, Qian, Li, Li, Luo & Li, 2024	*Suilla*-type	Present	Mou et al. 2024
43	*Murina yushuensis* Han, Csorba & Wu, 2024	*Suilla*-type	Present	Wang et al. 2024a

of cranium); **ZYW** = zygomatic width (greatest width of skull across zygomatic arches); **MAW** = mastoid width (greatest distance across mastoid region); **IOW** = interorbital width (least width of interorbital constriction); **CM^3L** = upper canine-molar length (from anterior of C^1 to posterior of M^3 crown); **C^1C^1W** = upper canine width (greatest width of outer borders of C^1); **M^3M^3W** = upper molar greatest width (greatest width of outer borders of M^3); **CM_3L** = lower canine-molar length (from anterior of C_1 to posterior of third lower molar (M_3) crown); **ML** = mandible length (from anterior rim of alveolus of I^2 to most posterior part of condyle); **MDL** = greatest length of mandible (from anterior point of first lower incisor (I^2) to most posterior part of condyle); **CPH** = coronoid process height (least distance from apex of coronoid process to indentation of lower border of ramus mandibula).

Principal component analysis (PCA) was employed to investigate the relative contributions of specific variables

to morphometric variation. Subsequently, cluster analysis was performed to group species based on the extracted principal components. For closely related species for which complete data were not available from the previously published literature, mean values were used for the subsequent analyses. All statistical analyses were conducted using SPSS v21.0 (SPSS, Inc., Chicago, IL, USA), and differences were considered statistically significant at a p-value of < 0.05.

DNA extraction, sequencing, and phylogenetic reconstruction

Genomic DNA was extracted from muscle tissue using a DNA extraction kit purchased from Tiangen Biotech (Beijing) Co., Ltd. In this study, we amplified and sequenced the mitochondrial COI and cytochrome b (Cyt *b*) genes from each DNA sample using the primers COI-F (5'-CCTACTCRGCCATTTTACCTATG-3'), COI-R (5'-ATCTCTGGGTGTCCAAAGAATCA-3'), Cytb-F (5'-ATGATATGAAAAACCATCGTTG-3'), and Cytb-R (5'-TTTCCNTTTCTGGTTTACAAGAC-3'). PCR amplification was performed with a 25-µl reaction volume under the following cycling conditions: an initial denaturing step at 95 °C for 5 min; 10 cycles of denaturing at 94 °C for 60 s, annealing at 46 °C for 30 s, and extension at 72 °C for 1 min; 25 cycles of denaturing at 94 °C for 60 s, annealing at 50 °C for 40 s, and extension at 72 °C for 1 min; 35 cycles of denaturing at 94 °C for 60 s, annealing at 54 °C for 40 s, and extension at 72 °C for 1 min; and a final extension at 72 °C for 10 min. The purified PCR products were sequenced using both forward and reverse primers with a BigDye Terminator Cycle Sequencing Kit according to the manufacturer's instructions. Sequencing was performed on an ABI Prism 3730 automated DNA sequencer manufactured by Chengdu TSING KE Biological Technology Co., Ltd. (Chengdu, China). All of the relevant sequences have been deposited in GenBank (Suppl. material 1: tables S2, S3).

Mitochondrial sequences were aligned in MEGA v7.0 (Kumar et al. 2016) using the MUSCLE algorithm (Edgar 2004) with default parameters. Phylogenetic trees were constructed using both maximum likelihood (ML) and Bayesian inference (BI) methods. The ML analysis was performed using IQ-tree v2.0.4 (Nguyen et al. 2015a) based on the best-fit model with 2000 ultrafast bootstrap (UFB) replicates (Hoang et al. 2018) and continued until a correlation coefficient of at least 0.99 was achieved. The BI analysis was performed using MrBayes v3.2.1 (Ronquist et al. 2012). Each BI analysis was run independently using four Markov Chain Monte Carlo chains (with three heated chains and one cold chain) starting with a random tree; each chain was then run for 6 million generations, and sampling was conducted every 1000 generations. Data run convergence was confirmed when the average standard deviation of split frequencies was less than 0.01. Nodes in the trees were considered well-supported when the Bayesian posterior probabilities were ≥ 0.95 (Ronquist et al. 2012) and the ML UFB value was $\geq 95\%$ (Hoang et al. 2018). The best-fit model for the BI and ML analyses was obtained based on the Bayesian information criterion computed with PartitionFinder v2.1.1 (Lanfear et al. 2017).

In the phylogenetic analysis, to elucidate the phylogenetic position of the new species within the genus *Murina* and the lineage relationships of the *M. huttoni* complex, we constructed three datasets: two COI datasets (*Murina*_1 and *Murina*_2) and one Cyt *b* dataset (*Murina*_3). *Murina*_1 comprises 92 sequences (657 bp), with 288 variable sites and 264 parsimony-informative sites. The evolutionary models for the first, second, and third codon positions were TIM+I+G, HKY+I, and TRN+I+G, respectively. *Murina*_2 includes 43 sequences (657 bp), with 188 variable sites and 142 parsimony-informative sites. The evolutionary models for the first, second, and third codon positions were TRNEF+G, F81+I, and TRN, respectively. *Murina*_3 consists of 46 sequences (1140 bp), with 506 variable sites and 448 parsimony-informative sites. The evolutionary models for the first, second, and third codon positions were K80+I+G, HKY+I+G, and TRN+I+G, respectively.

Species delimitation and genetic distance

To rapidly assess the boundaries of species currently recognized by taxonomists, we used a tree-based phylogenetic approach known as the multi-rate Poisson Tree Processes (mPTP) (Kapli et al. 2017). This method is comparatively more stable and widely used than other tree-based methods (e.g., GMYC and bPTP) (Blair and Bryson 2017). We used the ML tree generated by the COI sequences as input and performed the analysis on the mPTP web server (http://mptp.h.its.org) using the default parameters. Additionally, genetic distances were calculated based on COI and Cyt *b* sequences using the uncorrected p-distance model with 1,000 bootstrap replications in MEGA v7.0 (Kumar et al. 2016).

Results

Phylogeny and genetic divergence

Reconstructing the mitochondrial tree topology of Vespertilionidae based on the mitochondrial COI gene using both methods showed discordance (Fig. 2A and Suppl. material 1: fig. S1). The BI tree included monophyletic clades of the subfamilies Myotinae, Kerivoulinae, and Murininae, except for Vespertilioninae (Fig. 2A and Suppl. material 1: fig. S1), although the groups were not highly resolved. The monophyly of three genera of the subfamily Murininae, *Harpiocephalus*, *Harpiola*, and *Murina*, was not supported (Fig. 2A and Suppl. material 1: fig. S1), but could be further divided into four clades, Clades I–IV. Clade I consisted of only the single species *M. jinchui*; Clade II comprised *M. fanjingshanensis*,

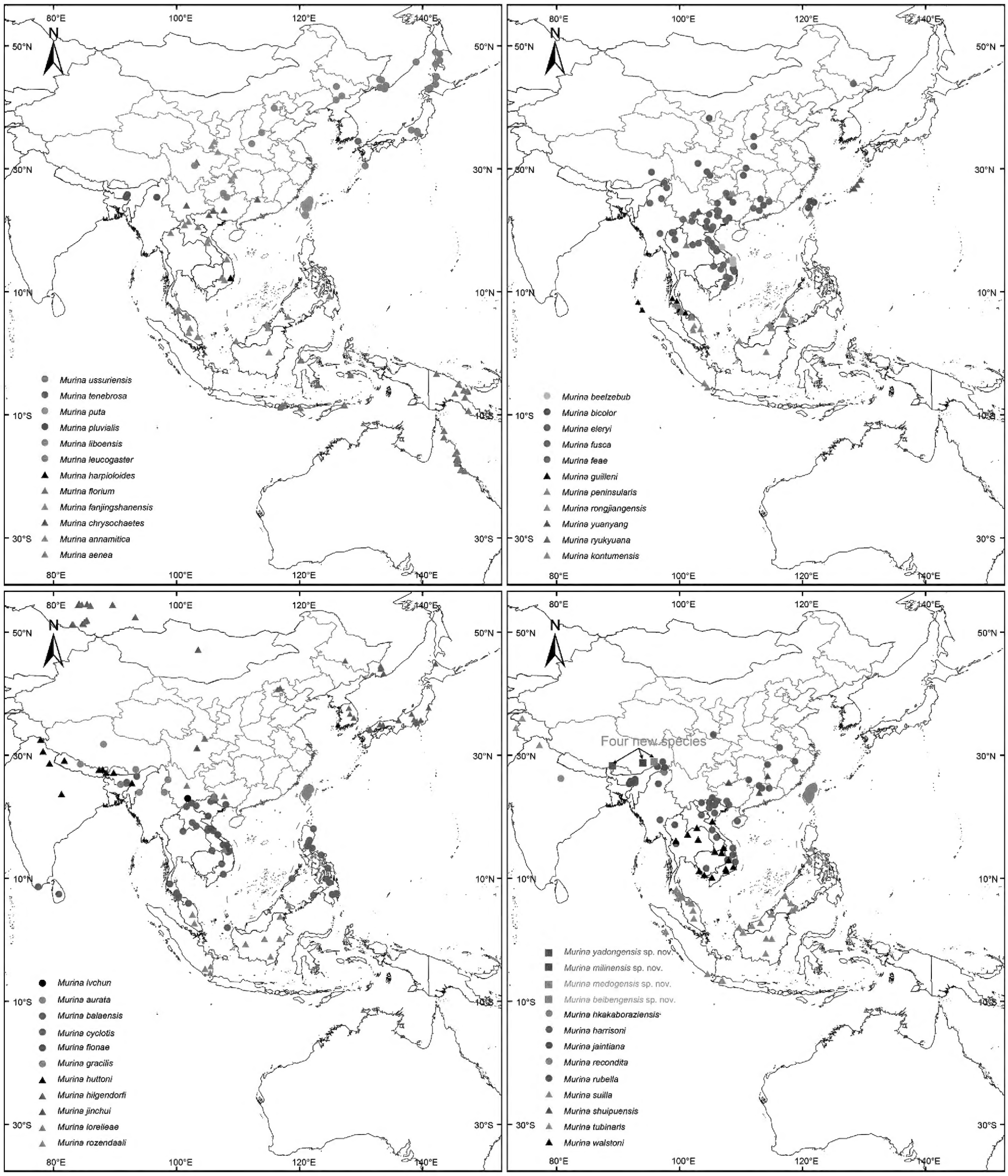

Figure 1. Geographical distribution of recognized species and the four new species of the genus *Murina* in Asia. The base maps are from the Standard Map Service website (http://bzdt.ch.mnr.gov.cn/index.html; Map Approval No. GS (2020) 4619).

M. rongjiangensis, *M. shuipuensis*, *M. leucogaster*, and *M. hilgendorfi*; Clade III contained the genus *Harpiola*, *M. harrisoni*, *M. ussuriensis*, and *M. huttoni*; and Clade IV comprised the remaining species, including four subclades, IV1–4, that were not highly supported (Fig. 2A and Suppl. material 1: fig. S1). However, phylogenetic analysis of mitochondrial Cyt *b* revealed *Harpiocephalus*, *Harpiola*, and *Murina* as independent monophyletic clades (Fig. 2B and Suppl. material 1: fig. S2).

Within subclade IV-1, a single specimen from Yadong County, Shigatse City, Xizang Autonomous Region, and three samples from Miling County, Nyingchi City, Xizang Autonomous Region, China, clustered together to become the sister clade of (*M. yushuensis* + (*M. harpioloides* + (*M. yuanyang* + *M. chrysochaetes*))) (Fig. 2A and Suppl. material 1: fig. S1). These two populations can be distinguished from the known species of the genus *Murina* and from the lineages undescribed in this study by morphological

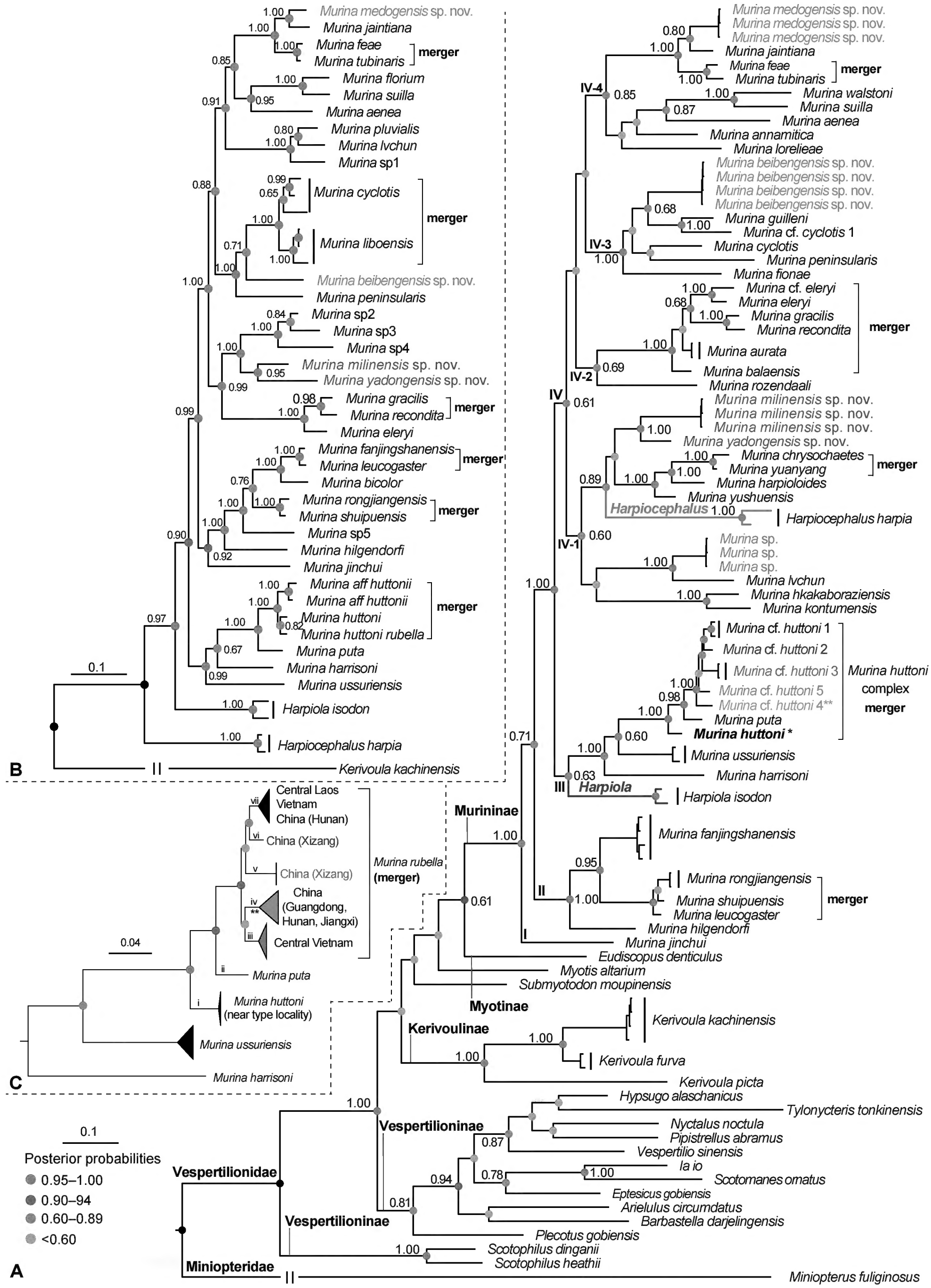

Figure 2. Phylogeny and species delimitation. **A.** BI tree and mPTP species delimitation based on mitochondrial COI; **B.** BI tree and mPTP species delimitation based on mitochondrial Cyt *b*; **C.** Bayesian tree and mPTP species delimitation in the *M. huttoni* complex. Scale bars represent 0.1/0.04 nucleotide substitutions per site. Taxa marked with "merger" indicate proposed merging schemes based on mPTP species delimitation results, while unmarked taxa are suggested as valid species.

characteristics (see subsequent comparisons) and molecular data, with *p*-distances of 12.2% (vs. *M. harpioloides*) and 10.8% (vs. *M. yushuensis*) (Suppl. material 3). These values are greater than the genetic distances between recognized species, e.g., 4.8% (*M. gracilis* vs. *M. recondita*) and 7.6% (*M. yushuensis* vs. *M. harpioloides*) (Suppl. material 3). Similarly, these two undescribed species formed independent lineages in the phylogeny reconstructed using Cyt *b* (Fig. 2B and Suppl. material 1: fig. S2), with the minimum genetic distances to congeners being 11.8% and 12.5%, respectively (Suppl. material 4). Thus, the populations at these two localities represent two independently evolved lineages, which are described below as two new species: *Murina yadongensis* sp. nov. and *Murina milinensis* sp. nov.

Within subclade IV-3, four samples from Beibeng Township, Medog County, Nyingchi City, and Xizang Autonomous Region, China, clustered together to form a sister clade to (*M. guilleni* + *M.* cf. *cyclotis* 1) and were highly supported (BPP/UFB = 0.95/95) (Fig. 2A and Suppl. material 1: fig. S1). This population can be distinguished from known species of the genus *Murina* and from lineages undescribed in this study by several morphological characters (see subsequent comparisons) and molecular differences, with a high *p*-distance of 12.0% (vs. *M. guilleni*) (Suppl. material 3). This is much greater than the genetic distances between recognized species, e.g., 9.7% (*M. hkakaboraziensis* vs. *M. kontumensis*) and 7.6% (*M. yushuensis* vs. *M. harpioloides*) (Suppl. material 3). In the phylogeny reconstructed using Cyt *b*, this population was resolved as a basal clade to *M. cyclotis* and *M. liboensis* (Fig. 2B and Suppl. material 1: fig. S2), with the minimum genetic distance to congeners being 11.8% (vs. *M. liboensis*) (Suppl. material 4). Thus, the population at this locality can be considered an independently evolved lineage and is described below as a new species, *Murina beibengensis* sp. nov.

Within subclade IV-4, three samples from Beibeng Township, Medog County, Nyingchi City, and Xizang Autonomous Region formed a distinct cluster and were highly supported as the sister clade to *M. jaintiana* (BPP/UFB = 0.95/99) (Fig. 2B and Suppl. material 1: fig. S1). This population can be distinguished from known species of the genus *Murina* and from lineages undescribed in this study by morphological characters (see subsequent comparisons) and molecular data, with a *p*-distance of 7.0% (vs. *M. jaintiana*) (Suppl. material 3). This value is greater than the genetic distances between recognized sister species, e.g., 4.5% (*M. feae* vs. *M. tubinaris*) (Suppl. material 1: table S4). In the phylogeny reconstructed using Cyt *b*, this population was resolved as the sister species to *M. jaintiana* (Fig. 2B and Suppl. material 1: fig. S2), with a minimum genetic distance of 6.1% between them (Suppl. material 4). Thus, the population at this locality represents an independently evolved lineage and is described below as a new species, *Murina medogensis* sp. nov.

Further phylogenetic analysis of expanded samples of the *M. huttoni* complex recovered seven clades (Fig. 2C), corresponding to those shown in Figure 2A, and published sequences of the subspecies *M. huttoni rubella* (Zhang et al. 2016) were nested within Clade IV (Fig. 2C). Within the *M. huttoni* complex, genetic distances ranged from 6.2% to 6.9%, which are much greater than the genetic distances between recognized species as previously described, e.g., 2.9% (*M. yuanyang* vs. *M. chrysochaetes*) (Suppl. material 1: table S7).

Species delimitation based on mitochondrial sequences

The mPTP species delimitation resolved the most recognized species and was generally consistent with the phylogenetic results. However, mPTP also suggested that five sets of recognized and undetermined species should be merged into a single species for each set: (1) *M. feae* + *M. tubinaris*; (2) *M.* cf. *eleryi* + *M. eleryi* + *M. gracilis* + *M. recondita* + *M. aurata* + *M. balaensis*; (3) *M. chrysochaetes* + *M. yuanyang*; (4) *M. rongjiangensis* + *M. shuipuensis* + *M. leucogaster*; and (5) *M.* cf. *huttoni* 1 + *M.* cf. *huttoni* 2 + *M.* cf. *huttoni* 3 + *M.* cf. *huttoni* 5 + *M.* cf. *huttoni* 4 + *M. puta* + *M. huttoni* (Fig. 2A). Species delimitation using mPTP based on Cyt *b* supported the results from COI-based delimitation but also suggested the merging of several species: (1) *M. feae* and *M. tubinaris*; (2) *M. cyclotis* and *M. liboensis*; (3) *M. gracilis* and *M. recondita*; (4) *M. fanjingshanensis* and *M. leucogaster*; (5) *M. rongjiangensis* and *M. shuipuensis*; and (6) the *M. huttoni* complex (Fig. 2B). However, since the sequences used were not entirely derived from type specimens, these results require further validation with additional evidence. In summary, the mPTP analyses supported the identification of the new species in this study as independent phylogenetic lineages.

The mPTP analysis suggested that *M.* cf. *huttoni* from central Laos, Vietnam, China (Hunan, Xizang, Guangdong, and Jiangxi), and central Vietnam be merged into a single species as the sister species of *M. puta* (Fig. 2C). Therefore, based on genetic and morphological differences, we propose to elevate its subspecies *M. h. rubella* to the species level. Detailed morphological comparisons are given below.

Morphological analyses

We measured 24 morphological characters from 17 specimens for PCA analysis. The number of morphological characters used for PCA analysis was not entirely consistent because data from the literature were incomplete. Overall, four undescribed new species were separated from closely related species in the PCA plots.

For *M. beibengensis* sp. nov., *M. guilleni*, *M. cyclotis*, and *M. peninsularis*, a total of three principal components were extracted from the 20 traits. The first three principal components explained 90.16% of the total variation (Suppl. material 1: table S8). In the PCA plot, the cluster formed by a single sample of *M. beibengensis* sp. nov. was clearly separated from the remaining three species along the PC1 axis, which was loaded with all traits (Fig. 3A).

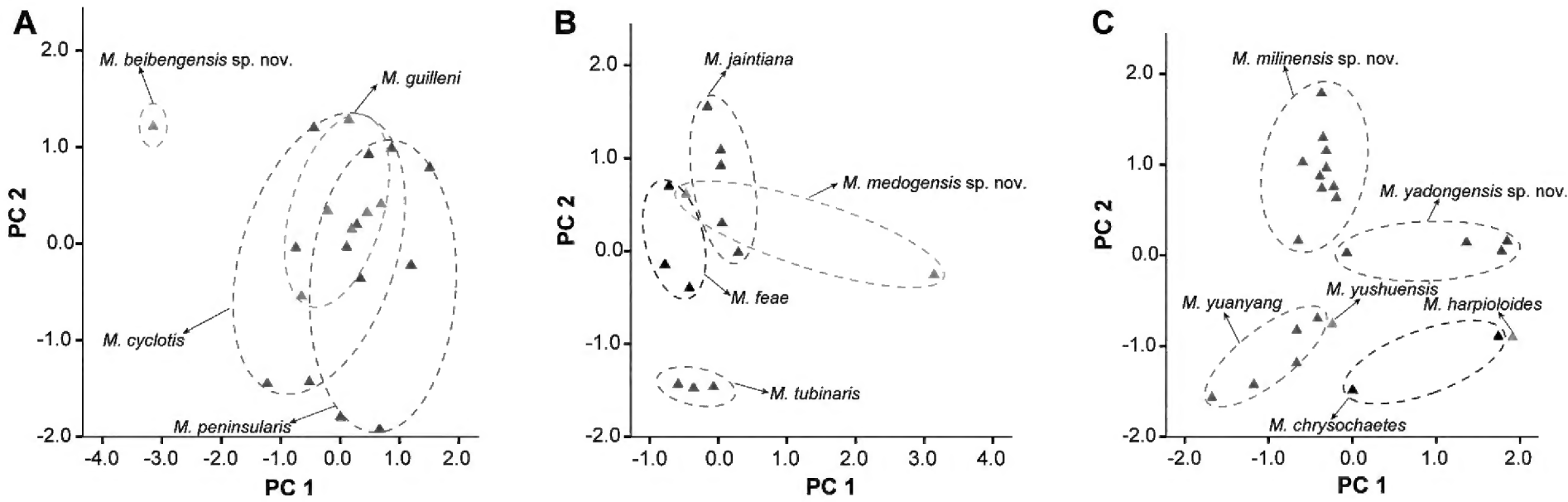

Figure 3. Plots of principal component analysis for the four new species and closely related species, based on morphological characters.

For *M. medogensis* sp. nov., *M. jaintiana*, *M. feae*, and *M. tubinaris*, three principal components were extracted from the 15 traits. PC1 and PC2 explained 18.85% and 16.53% of the total variance, respectively (Suppl. material 1: table S9). In the PCA plot, *M. medogensis* sp. nov. showed slight overlap with *M. jaintiana* and *M. feae* but was separated along the PC1 axis, forming a distinct cluster comprising a single sample (Fig. 3B).

For *M. milinensis* sp. nov., *M. yadongensis* sp. nov., *M. chrysochaetes*, *Murina yuanyang*, *M. harpioloides*, and *M. yushuensis*, a total of eight principal components were extracted. The first two principal components explained 50.14% of the total variance (Suppl. material 1: table S10). In the PCA plot, *M. milinensis* sp. nov. and *M. yadongensis* sp. nov. formed two distinct and independent clusters, which were separated from the remaining species along the PC2 axis (Fig. 3C). Traits loaded on the PC2 axis included FA, TIB, skull, and ear measurements (Suppl. material 1: table S10).

Based on mitochondrial and morphological differences, the four populations of *Murina* from the Xizang Autonomous Region, China, represent four new undescribed species. We formally describe them in what follows.

Taxonomic account

Murina beibengensis Luo, Mao & Zhou, sp. nov.

https://zoobank.org/A92D812D-B160-4242-A9D9-49752EBBC79F

Figs 4, 5, Table 2, Suppl. material 2

Holotype. • Adult male, field number XZ2024037 (Figs 4, 5, Table 2), collected by Tao Luo, Ming-Le Mao, Chang-Ting Lan, Zi-Fa Zhao, and Zhong-Lian Wang on 15 August 2024, from Beibeng Township, Medog County, Nyingchi City, Xizang Autonomous Region, China (29.22926454°N, 95.15008271°E; ca. 864 m. a.s.l.; Fig. 1).

Measurements (in mm) and body mass (in g) of the holotype. HB: 43.25, EL: 16.18, EW: 8.61, TRL: 8.67, TRW: 2.29, HFL: 8.64, FL: 31.94, TIB: 18.42, GTL: 15.68, CCL: 12.50, BCW: 7.57, BCH: 7.78, ZYW: 8.20, MAW: 7.58, IOW: 4.24, CM^3L: 4.98, C^1C^1W: 3.65, M^3M^3W: 4.61, RCM: 0.79, CM_3L: 5.92, ML: 11.52, MDL: 11.98, CPH: 4.38; BW: 6.20.

Etymology. The specific epithet *beibengensis* refers to the type locality of the new species: Beibeng Township, Medog County, Nyingchi City, Xizang Autonomous Region, China. We propose the common English name "Beibeng Tube-nosed Bat" and the Chinese name "Bèi Bēng Guǎn Bí Fú (背崩管鼻蝠)".

Diagnosis. *Murina beibengensis* sp. nov. can be distinguished from all other congeners by the following combination of characters: (1) small-size *Murina*, FL 31.94 mm, GTL 15.68 mm; (2) dorsal fur orangish-yellow overall, grey at the base, gradually transitioning to orange-yellow tips halfway from the base; (3) ventral fur silvery-gray overall, dark grey at the base, with silvery-gray tips; (4) ears broadly rounded, with smoothly convex anterior margins, no notch on posterior margins; (5) forearm and wrists covered with sparse hairs; (6) wing attachment point located at 1/3 from base of claw to base of toe; (7) sagittal and lambdoid crests well developed; (8) I^2 is situated laterally anterior to I^3 and partially visible in the lateral view, and I^2 slightly taller than I^3; (9) mesostyles of M^1 and M^2 are reduced; (10) C^1 taller than P^4, P^2 smaller than P^4 in height, and crown area of P^2 larger than 2/3 that of P^4; (11) P_2 approximately equal to P_4 in height, with a basal area 2/3 that of P_4; (12) C_1 larger than P_4 in height and basal area; (13) mandibular foramina clearly visible, situated below P_2.

Description. Morphometric data of *Murina beibengensis* sp. nov. are provided in Table 2 and Suppl. material 2. Small-size *Murina*, HB 43.25 mm, FL 31.94 mm, EL 16.18 mm, HFL 8.64 mm, and BW 6.20 g. Nostrils tubular, open sideways, and slightly short. Ears small, short, oval, blunt at tips, with smoothly convex anterior margins, not notched on posterior margin. Tragus short, narrow, and tapering toward a pointed tip, with slightly convex anterior margin, concave posterior margin, and basal notch, and slightly curved outward, about half as long as ear. Body covered with thick and fluffy hair. Dorsal hairs orangish-yellow overall (bicolored, grayish black at the base, gradually transitioning to orange-yellow tips halfway from base). Dorsal hairs extend onto bases of wings; uropatagium, thumbs, forearm, wrist, tibia, and feet, with

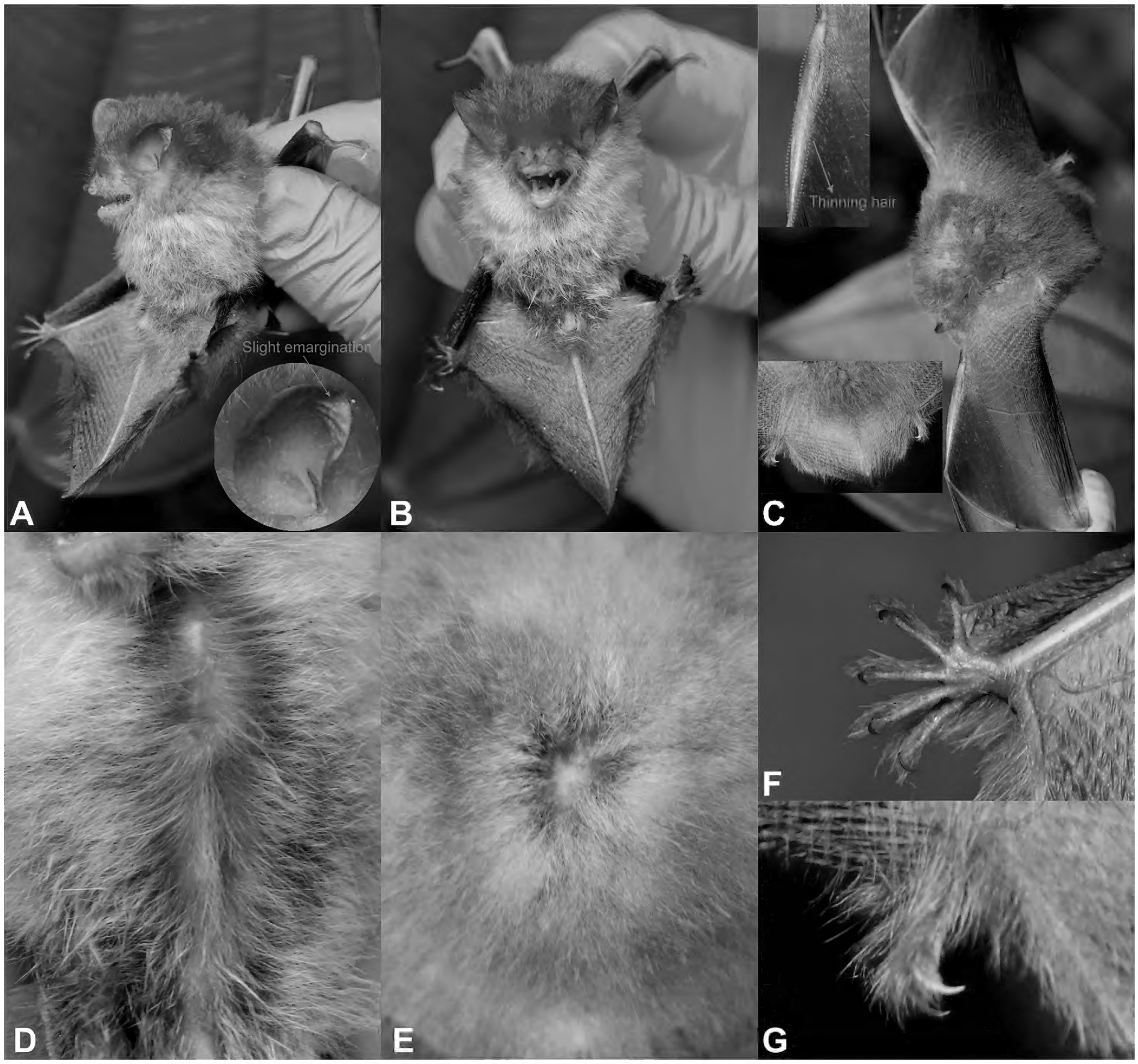

Figure 4. External morphological characteristics of *Murina beibengensis* sp. nov. in living holotype, XZ2024037. **A.** Lateral view; **B.** Ventral view; **C.** Dorsal view of the body and uropatagium; **D.** Ventral hairs; **E.** Dorsal hairs; **F.** Hindfoot ventral view; **G.** Hindfoot dorsal view.

well-developed fringe of hairs around margin of uropatagium. Densely furred anterior 1/3 of the dorsal uropatagium, posterior 2/3 covered with sparse hairs. Ventral hairs are silvery-gray overall, tricolored, gray-white at the base, central dark gray, with silvery-gray tips. Flesh purple around the eyes, muzzle, and lower forehead, and the face is hairy except for the long, protuberant nostrils that are naked. TL 32.69 mm, tip of the tail extending significantly past the rear edge of the uropatagium, tip slightly free. Plagiopatagium attachment point located at the middle of the claw of the first toe.

Skull robust and domed, relatively small, GTL 15.68 mm. Rostrum long, deep, gradually ascending to forehead; prominent median depression present. Sagittal and lambdoid crests well developed. In dorsal view, braincase nearly rounded; zygomatic arches weak and slender, gradually widening posteriorly, widest at the base of the zygomatic arches; posterior margin of skull not protruding; middle from snout to frontal region distinctly concave downward. In lateral view, skull slightly elongated, with elongated oval braincase; height gradually rising from snout to parietal, with slightly increasing slope from snout to frontal and decreasing slope from frontal to parietal; slight depression between snout and frontal, without distinct prominence at frontal; zygomatic arches gradually rising from anterior to posterior, highest at the middle of zygomatic arches. In ventral view, palatine wide and nearly flat, ending at midpoint of C^1; basisphenoid pits slightly shallowly teardrop-shaped, extending posteriorly to anterior third of cochlea. Mandible length 11.52 mm, inverted L-shaped. Line between coronoid process and condyle nearly flat; distinct inward depression between condyle and angle; angle slightly long and wide; mandibular foramina clearly visible, situated below P_2.

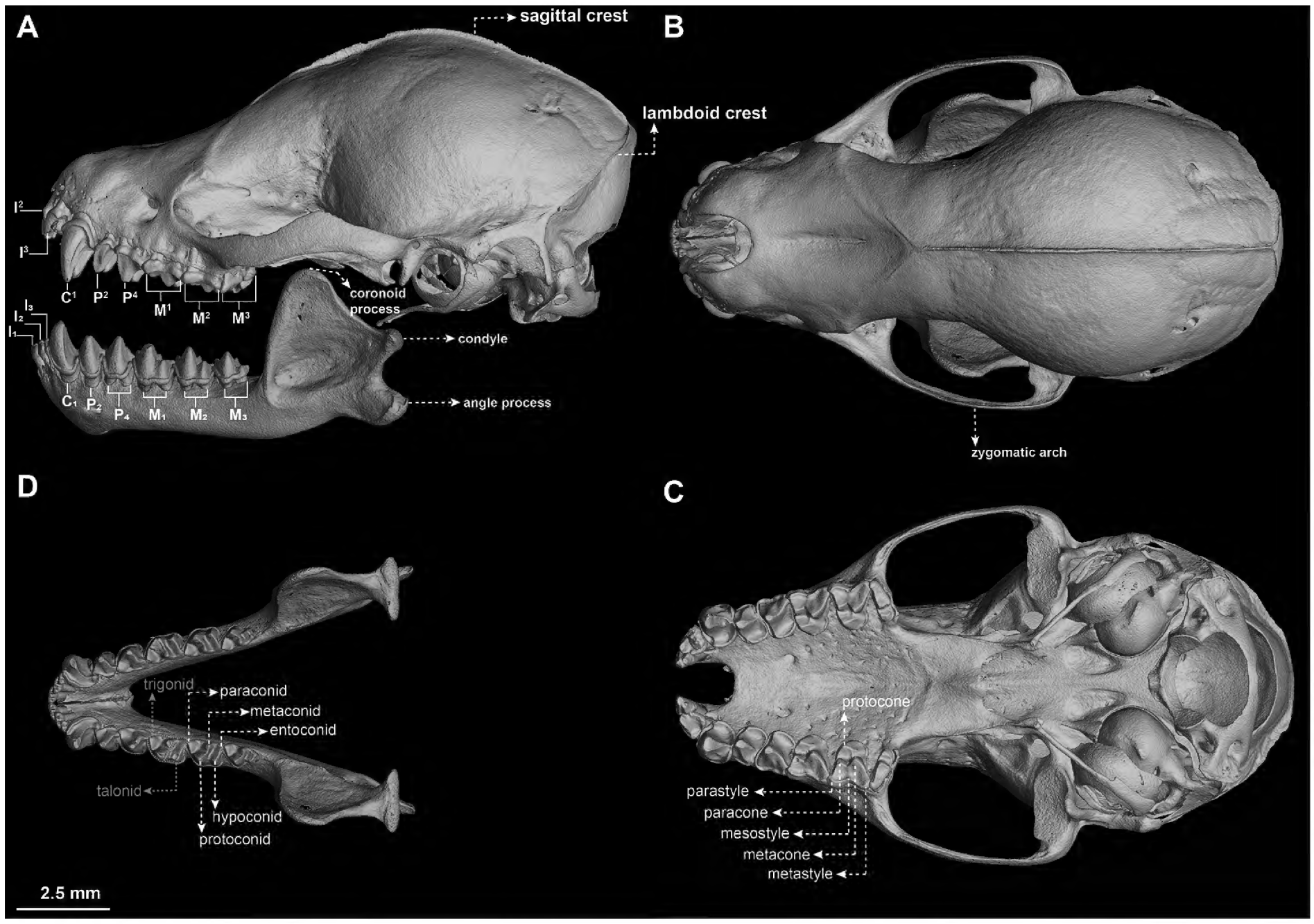

Figure 5. Micro-CT reconstruction of the skull of *Murina beibengensis* sp. nov. holotype, XZ2024037. **A.** Lateral view; **B.** Dorsal view; **C.** Ventral view; **D.** Frontal view of mandible.

Dental morphology: Dental formula is I2/3, C1/1, P2/2, M3/3=34 (Fig. 5). In the maxilla, I^2 is situated laterally anterior to I^3 and partially visible in the lateral view; the crown area of P^2 larger than 2/3 that of P^4 and smaller than that of C^1. Based on these characters, the species belongs to the "*cyclotis*-type". Maxillary dentition converges slightly anteriorly (RCM = 0.79). I^2 and I^3 bicuspid, smaller secondary cusp situated posterior to primary cusp; I^2 is slightly taller than I^3, with a crown area half that of I^3; distinct gap between posterior of I^3 and C^1, not in contact, about 1/3 of height of C^1. C^1 taller than P^4, slightly elongated and lacking secondary cusps, crown area approximately equal to P^4; P^2 is slightly smaller, delicate and pointed, about 4/5 as high as P^4 and 2/3 as high as C^1, crown area of P^2 is 2/3 that of P^4. Mesostyles of M^1 and M^2 are reduced, but retaining distinct cusps; paracone, protocone, metacone, and parastyle well developed. M^3 are reduced, with only parastyle, paracone, and protocone. In the mandible, the first, second, and third lower incisors (I_1, I_2, and I_3) smaller, tricuspid, nearly equal in height and width; slight overlap of outer cusps of I_1, I_2, and I_3 with gradual increase in height from I_1 to C_1. C_1 contains pointed cusp on anterior inner margin, in contact with I_3 outer cusp, exceeding P_2 and P_4 in height and basal area; C_1 larger than P_4 in height and basal area. P_2 nearly equal to P_4 in height, and the basal and crown area of P_2 approximately 2/3 that of P_4. In lateral view, trigonids of M_1, M_2, and M_3, metaconid, and paraconid approximately 2/3 as high as protoconid. Talonids of M_1 and M_2 are approximately half the size of trigonids; entoconid and hypoconid distinctly separated from trigonid, nearly equal to metaconid and paraconid in height. M_1 and M_2 are nyctalodont types, with well-developed entoconids. M_3 reduced, talonid approximately 1/3 as long as trigonid, paraconid, protoconid, and metaconid complete and well developed.

Morphological comparisons with congeneric species. Based on its dentition, I^2 is situated laterally anterior to I^3, and I^2 is partially visible in the lateral view, and crown area of P^2 larger than 2/3 that of P^4, *Murina beibengensis* sp. nov. belongs to the "*cyclotis*-type" a character that distinguishes 30 species belonging to the "*suilla*-type", I^2 is anterior to I^3, I^2 is clearly visible in the lateral view, and the crown area of P^2 is half or less than that of P^4, including *M. rubella*, *M. aurata*, *M. balaensis*, *M. beelzebub*, *M. bicolor*, *M. chrysochaetes*, *M. eleryi*, *M. fanjingshanensis*, *M. feae*, *M. fusca*, *M. gracilis*, *M. harpioloides*, *M. hilgendorfi*, *M. hkakaboraziensis*, *M. jaintiana*, *M. jinchui*, *M. kontumensis*, *M. leucogaster*, *M. liboensis*, *M. lorelieae*, *M. rongjiangensis*, *M. ryukyuana*, *M. shuipuensis*, *M. suilla*, *M. tenebrosa*, *M. tubinaris*, *M. ussuriensis*, *M. walstoni*, *M. yuanyang*, and *M. yushuensis*. Detailed morphological differences between the new species and congeners are listed in Suppl. material 5 and illustrated in Suppl. material 1: fig. S3.

Table 2. External and craniodental measurements (in mm) of *M. beibengensis* sp. nov. and three closely related species. NA indicates that the data is not available.

Species	*M. beibengensis* sp. nov.	*M. guilleni* (Soisook et al. 2013a)			*M. cyclotis* (Soisook et al. 2013a)		*M. peninsularis* (Soisook et al. 2013a)	
	Holotype (Female)	Holotype (Male)	Male (n = 6)	Female (n = 3)	Male (n = 36)	Female (n = 40)	Male (n = 23)	Female (n = 19)
BW	6.20	6.50	NA	NA	NA	NA	NA	NA
HB	43.25	48.00	43.2–51.6 (48.0 ± 3.2)	48.0–48.3 (48.2 ± 0.2)	38.7–46.4 (42.3 ± 2.3)	41.1–50.0 (45.1 ± 2.8)	39.9–50.1 (46.6 ± 3.0)	42.0–55.1 (49.9 ± 3.7)
TL	32.69	35.20	28.1–39.2 (35.9 ± 4.0)	35.9–42.0 (39.1 ± 3.1)	26.2–39.0 (34.9 ± 3.9)	32.0–41.1 (37.4 ± 2.5)	32.4–42.8 (38.7 ± 3.3)	38.5–46.0 (42.3 ± 1.9)
EL	16.18	12.60	11.4–15.2 (13.7 ± 1.4)	13.5–15.1 (14.4 ± 0.8)	12.0–17.6 (14.0 ± 1.3)	12.7–16.0 (14.5 ± 1.0)	11.9–18.8 (14.2 ± 1.7)	13.0–17.0 (15.1 ± 1.2)
EW	8.61	NA	NA	NA	NA	NA	NA	NA
TRL	8.67	NA	8.30–9.20 (8.6 ± 0.5)	NA	6.80–9.30 (8.1 ± 0.6)	5.80–9.20 (7.9 ± 0.9)	7.40–10.30 (8.4 ± 0.9)	7.60–9.00 (8.3 ± 0.5)
TRW	2.29	NA	NA	NA	NA	NA	NA	NA
HFL	8.64	8.10	7.7–9.4 (8.5 ± 0.6)	8.0–8.4 (8.2 ± 0.2)	6.5–8.8 (7.9 ± 0.6)	7.0–9.7 (8.3 ± 0.8)	5.6–9.1 (7.8 ± 0.9)	7.1–10.0 (9.0 ± 0.8)
FL	31.94	34.00	31.9–34.0 (33.2 ± 0.7)	35.0–35.9 (35.4 ± 0.5)	29.4–33.0 (30.7 ± 0.9)	31.6–36.8 (33.9 ± 1.0)	33.8–38.1 (35.7 ± 1.3)	34.5–39.4 (37.7 ± 1.2)
TIB	18.42	19.60	17.7–19.7 (18.4 ± 0.8)	18.1–19.7 (18.9 ± 0.8)	14.5–19.3 (17.6 ± 1.1)	17.3–20.3 (17.6 ± 1.1)	18.2–21.6 (19.5 ± 1.0)	11.1–21.0 (19.3 ± 2.5)
GTL	15.68	17.03	16.40–17.54 (17.10 ± 0.43)	17.12–18.10 (17.65 ± 0.50)	15.86–17.08 (16.47 ± 0.34)	16.6–18.18 (17.21 ± 0.47)	17.39–18.52 (17.79 ± 0.31)	17.59–19.33 (18.70 ± 0.52)
CCL	12.50	14.88	14.47–15.19 (14.85 ± 0.26)	15.09–15.76 (15.43 ± 0.34)	13.60–15.12 (14.45 ± 0.34)	14.34–16.17 (15.22 ± 0.41)	14.90–16.41 (15.52 ± 0.41)	15.53–16.89 (16.40 ± 0.36)
BCW	7.57	7.74	7.65–7.82 (7.76 ± 0.06)	7.53–7.74 (7.64 ± 0.11)	7.16–8.10 (7.64 ± 0.22)	7.40–8.17 (7.71 ± 0.19)	7.72–8.48 (8.12 ± 0.19)	7.70–8.58 (8.22 ± 0.22)
BCH	7.87	6.57	6.57–6.91 (6.68 ± 0.12)	6.78–7.10 (6.94 ± 0.16)	6.08–7.22 (6.49 ± 0.30)	6.10–7.21 (6.5 ± 0.24)	6.79–8.22 (7.32 ± 0.32)	7.10–8.37 (7.48 ± 0.34)
ZYW	8.20	9.72	9.29–9.93 (9.60 ± 0.22)	9.75–10.02 (9.92 ± 0.15)	8.78–10.05 (9.36 ± 0.31)	9.33–10.43 (9.84 ± 0.29)	9.76–11.31 (10.36 ± 0.38)	10.12–11.22 (10.80 ± 0.27)
MAW	7.58	8.15	8.00–8.28 (8.12 + 0.11)	8.18–8.43 (8.34 ± 0.14)	7.11–8.48 (7.90 ± 0.26)	7.64–8.58 (8.20 ± 0.21)	8.32–9.39 (8.74 ± 0.27)	8.08–9.62 (9.02 ± 0.34)
IOW	4.24	4.31	4.24–4.44 (4.34 ± 0.07)	4.20–4.44 (4.32 ± 0.12)	3.92–4.48 (4.17 ± 0.12)	3.99–4.52 (4.25 ± 0.13)	4.31–4.97 (4.57 ± 0.19)	4.46–4.88 (4.68 ± 0.12)
CM^3L	4.98	5.44	5.44–5.72 (5.58 ± 0.12)	5.50–5.91 (5.67 ± 0.21)	5.12–5.68 (5.41 ± 0.15)	5.06–6.00 (5.61 ± 0.19)	5.52–6.09 (5.76 ± 0.18)	5.68–6.39 (6.07 ± 0.18)
C^1C^1W	3.65	4.16	4.12–4.31 (4.19 ± 0.07)	4.28–4.44 (4.34 ± 0.09)	3.73–4.27 (4.00 ± 0.14)	4.00–4.67 (4.25 ± 0.14)	4.28–5.28 (4.66 ± 0.25)	4.46–5.26 (4.97 ± 0.17)
M^3M^3W	4.61	5.80	5.36–5.80 (5.54 ± 0.16)	5.68–5.87 (5.79 ± 0.10)	5.07–5.79 (5.39 ± 0.18)	5.18–6.05 (5.57 ± 0.19)	5.45–6.22 (5.72 ± 0.18)	5.69–6.20 (5.94 ± 0.15)
RCM	0.79	0.72	NA	NA	NA	NA	NA	NA
CM_3L	5.92	6.00	5.83–6.12 (6.00 ± 0.09)	6.01–6.43 (6.18 ± 0.22)	5.57–6.18 (5.84 ± 0.14)	5.75–6.49 (6.11 ± 0.16)	5.94–8.02 (6.31 ± 0.42)	6.28–6.94 (6.55 ± 0.21)
ML	11.52	11.43	11.13–11.74 (11.38 ± 0.21)	11.95–12.34 (12.11 ± 0.21)	10.52–11.68 (11.17 ± 0.30)	11.32–12.78 (11.86 ± 0.35)	11.25–12.92 (11.92+0.39)	12.09–13.59 (12.75 ± 0.41)
MDL	11.98	NA	NA	NA	NA	NA	NA	NA
CPH	4.38	4.78	4.33–4.93 (4.63 ± 0.21)	5.05–5.15 (5.10 ± 0.05)	3.77–4.60 (4.14 ± 0.21)	4.16–5.30 (4.71 ± 0.27)	4.30–5.33 (4.86 ± 0.29)	4.72–6.08 (5.51 ± 0.39)

Within the "*cyclotis*-type", *Murina beibengensis* sp. nov. can be distinguished from *M. aenea*, *M. fionae*, *M. harrison*i, *M. huttoni*, *M. peninsularis*, and *M. puta* by the forearm length 31.94 mm (vs. forearm length over 33 mm); from *M. annamitica*, *M. pluvialis*, and *M. recondita* by lacking off-white circumferential band around the neck (vs. present); from *M. cyclotis* and *M. guilleni* by the very well-developed sagittal and lambdoid crests (vs. poorly developed); and from *M. rozendaali* by ventral fur silvery-gray overall (vs. yellowish white) and mesostyles of M^1 and M^2 moderately reduced (vs. well-developed).

M. florium, which is not assigned to either the "*suilla*-type" or "*cyclotis*-type", can be distinguished by the following morphological characters: P^2 is 2/3 the height of P^4 (vs. P^2 equal to P^4), and the mesostyles of M^1 and M^2 are reduced (vs. well-developed).

Habitat and ecology. The new species is only found in two areas of Xizang, China. The type specimen was captured in a broad-leaved evergreen forest near Beibeng Township, Medog County, Nyingchi City, Xizang Autonomous Region, China (about 2.8 km from the town center) using a harp net. The type locality has a subtropical

climate with a mean annual temperature of 16 °C and mean annual precipitation of 2500–3900 mm. The site is surrounded by several cash crops (e.g., tea trees and bananas). In addition, two *Rhinolophus* sp., six *Hipposideros armiger*, three *H. pratti*, and one *Cynopterus sphinx* were captured here and in the surrounding area. Another distribution site in a cave near Riduo Township, Maizhokunggar County, Lasa City, and Xizang Autonomous Region yielded two carcasses. This site has a highland temperate semi-arid monsoon climate, with a mean annual temperature of 0.8 °C, mean annual precipitation of 350 mm, and sparse surrounding vegetation. Accordingly, we hypothesize that this new species may have a wider distribution in the Qinghai-Xizang Plateau.

Remark. Two genetic samples, field numbers XZ2024B05 and XZ2024B12, gender unknown, collected from a cave near Riduo Township, Maizhokunggar County, Lasa City, and Xizang Autonomous Region, China (29.69274086°N, 92.24386096°E, 4414 m) on 12 August 2024. These two samples occurred as dry and decomposed carcasses; no morphological data could be obtained, and only muscle tissue was preserved for sequencing.

Murina medogensis Mao, Lan & Zhou, sp. nov.

https://zoobank.org/FBCAA154-2DD4-48E1-B7E6-14333EB44047

Figs 6–9, Table 3, Suppl. material 2

Holotype. • Adult male, field number XZ2024038 (Figs 6, 7), collected by Ming-Le Mao, Tao Luo, Chang-Ting Lan, Zi-Fa Zhao, and Zhong-Lian Wang on 16 August 2024, from Medog Town, Medog County, Nyingchi City, Xizang Autonomous Region, China (29.29867524°N, 95.28785706°E; ca. 813 m. a.s.l.; Fig. 1).

Paratype. • Field number XZ2024006 (Figs 8, 9), adult female, collected near Beibeng Township, Medog County, Nyingchi City, Xizang Autonomous Region, China (29.2297514°N, 95.14752388°E; ca. 816 m) on 14 August 2024.

Measurements (in mm) and body weight (in g) of the holotype. HB: 38.46, EL: 11.89, EW: 6.79, TRL: 6.19, TRW: 1.94, HFL: 6.94, FL: 29.75, TIB: 15.47, GTL: 15.01, CCL: 14.09, BCW: 7.55, BCH: 6.71, ZYW: 8.74, MAW: 7.11, IOW: 4.39, CM^3L: 4.82, C^1C^1W: 3.61, M^3M^3W: 5.07, RCM: 0.712, CM_3L: 5.86, ML: 9.1, MDL: 10.21, CPH: 3.42; BW: 4.20.

Etymology. The specific epithet *medogensis* refers to the type locality of the new species: Medog Town, Medog County, Nyingchi City, Xizang Autonomous Region, China. We propose the common English name "Medog Tube-nosed Bat" and the Chinese name "Mò Tuō Guǎn Bí Fú (墨脱管鼻蝠)".

Diagnosis. *Murina medogensis* sp. nov. can be distinguished from all of the other congeners by the following combination of characters: (1) small-size *Murina*, FL 29.75–31.24 mm, GTL 15.01–18.74 mm; (2) dorsal fur dark grayish overall, dark grey at the base, gradually transitioning to gray-brown/white tips 2/3 from the base; (3) ventral fur silvery-gray overall, dark grey at the base, with silvery-gray tips; (4) ears broadly rounded, with smoothly convex anterior margins, no notch on posterior margins; (5) forearm and wrists without covered sparse hairs; (6) wing attachment point located at 1/3 from base of claw to base of toe; (7) sagittal crest absent, lambdoid crest present and poorly developed; (8) I^2 is situated laterally anterior to I^3 and partially visible in the lateral view, I^2 equal to I^3 in height; (9) mesostyles of M^1 and M^2 are well developed; (10) C^1 slightly lower than P^4 in height and crown area of P^2 larger than 2/3 that of P^4; (11) P^2 is approximately equal to P^4 in height, with a basal area 2/3 that of P^4; (12) C_1 taller than P_4 in height, crown area equal to P_2 and 2/3 of P_4; (13) mandibular foramina clearly visible, situated below P_4; (14) without distinct prominence at frontal aspect of skull.

Description. Morphometric data of *Murina medogensis* sp. nov. are provided in Table 3 and Suppl. material 2. Small-size *Murina*, HB 37.68–38.46 mm, FL 29.75–31.24 mm, EL 11.89–14.06 mm, HFL 6.94–8.52 mm, and BW 4.20 g. Nostrils tubular, open sideways, and slightly short. Ears small, short, oval, blunt at tips, with smoothly convex anterior margins, not notched on posterior margin. Tragus short, narrow, and tapering toward pointed tips, with slightly convex anterior margin, concave posterior margin, and basal notch, and it curves outwards slightly, about half as long as ear. Body covered with thick and fluffy hair. Dorsal hairs dark grayish overall (bicolored, dark grey at the base, gradually transitioning to gray-brown/white tips 2/3 from base). Dorsal hairs extend onto bases of wings, uropatagium, thumbs, tibia, and feet, with slight-developed fringe of hairs around margin of uropatagium. Densely furred anterior 1/3 of the dorsal uropatagium, posterior 2/3 covered with sparse hairs. Ventral hairs are silvery-gray overall, bicolored, dark grey at the base, with silvery-gray tips. Flesh-purple around the eyes, muzzle, and lower forehead, and the face is hairy except for the long, protuberant nostrils that are naked. TL 34.54–36.37 mm, slightly shorter than head-body length, tip of the tail extending significantly past the rear edge of the uropatagium, tip slightly free. Plagiopatagium attachment point located at about 1/3 from base of claw to base of toe, near base of claw (Fig. 6F, G).

Skull robust and domed, relatively small, GTL 15.01–18.74 mm. Rostrum long, deep, gradually ascending to forehead; prominent median depression present. Sagittal crest absent, lambdoid crest present, poorly developed. In dorsal view, braincase nearly rounded; zygomatic arches weak and slender, gradually widening posteriorly, widest at the base of the zygomatic arches; posterior margin of skull slightly protruding; middle from snout to frontal region distinctly concave downward. In lateral view, skull slightly elongated, with elongated oval braincase; height gradually rising from snout to parietal, with slightly increasing slope from snout to frontal and decreasing slope from frontal to parietal; slight depression between snout and frontal, without distinct prominence at frontal; zygomatic arches gradually rising from anterior to posterior. In ventral view, palatine wide and nearly flat, ending at

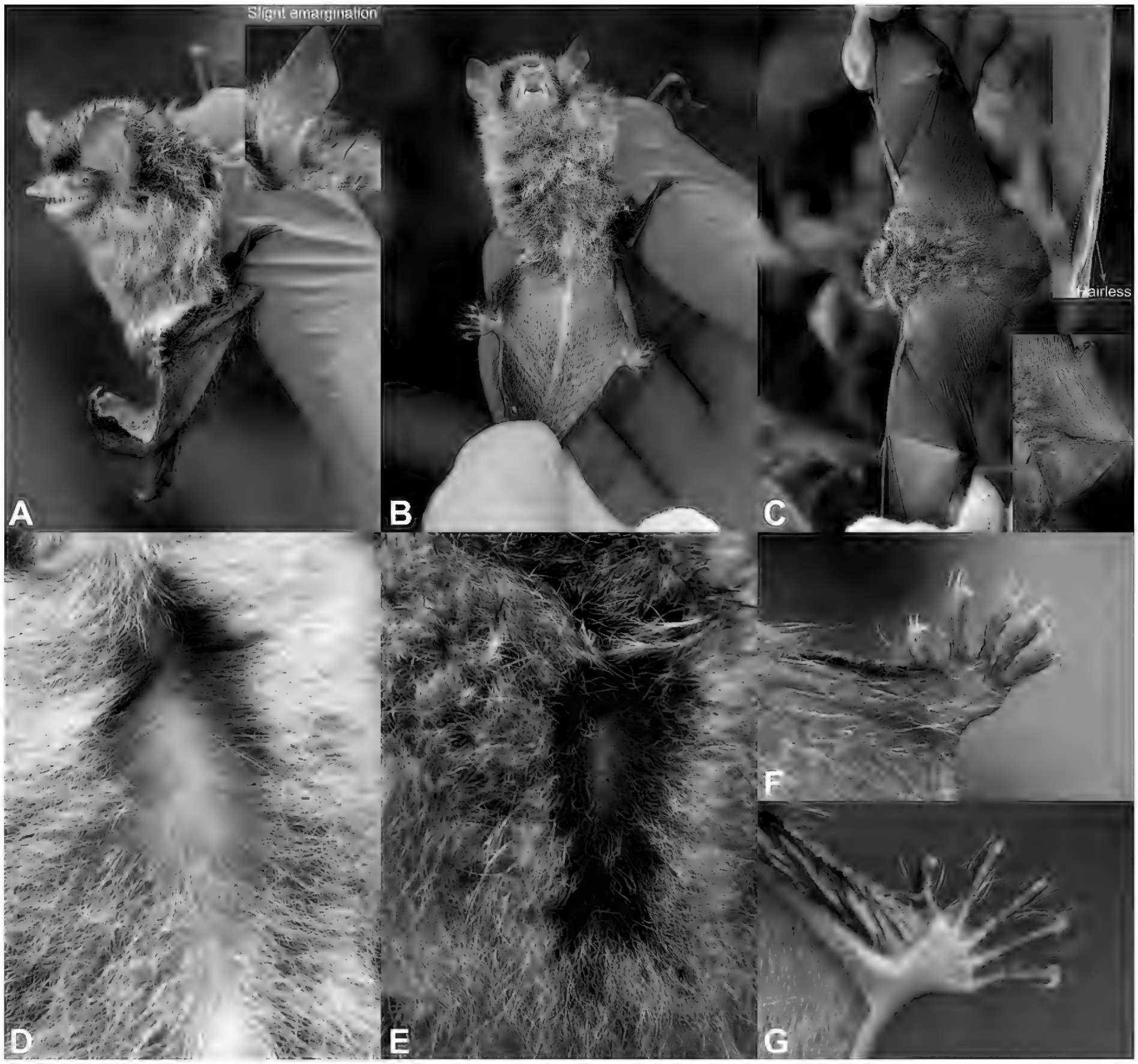

Figure 6. External morphological characteristics of *Murina medogensis* sp. nov. in living holotype, XZ2024038. **A.** Lateral view; **B.** Ventral view; **C.** Dorsal view of the body and uropatagium; **D.** Ventral hairs; **E.** Dorsal hairs; **F.** Hindfoot ventral view; **G.** Hindfoot dorsal view.

posterior margin of C^1; basisphenoid pits slightly shallowly teardrop-shaped, extending posteriorly to anterior third of cochlea. Mandible length 9.1 mm, inverted L-shaped. Line between coronoid process and condyle nearly flat; distinct inward depression between condyle and angle; angle slightly long and wide; mandibular foramina clearly visible, situated below P_4.

Dental morphology: Dental formula is I2/3, C1/1, P2/2, M3/3=34 (Figs 7, 8). In the maxilla, I^2 is situated laterally anterior to I^3 and partially visible in the lateral view; crown area of P^2 larger than 2/3 that of P^4 and smaller than that of C^1. Based on these characters, the species belongs to the "*cyclotis*-type". Maxillary dentition converges slightly anteriorly (RCM = 0.71). I^2 and I^3 bicuspid, smaller secondary cusp situated posterior to primary cusp; I^2 equal to I^3 in height, crown area of I^2 less than half that of I^3; distinct gap between posterior surface of I^3 and C^1, not in contact, about half of height of C^1. C^1 slightly lower than P^4 in height, slightly elongated and lacking secondary cusps, crown area 2/3 that of P^4; P^2 slightly smaller, delicate and pointed, about half as high as P^4 and 2/3 as high as C^1, crown area 2/3 that of P^4. Mesostyles of M^1 and M^2 are reduced, but retaining distinct cusps; paracone, protocone, metacone, and parastyle well developed. M^3 reduced, with only parastyle, paracone, and protocone. In the mandible, I_1, I_2, and I_3 smaller, tricuspid, almost equal in height and width; slight overlap of outer cusps of I_1, I_2, and I_3; with gradual increase in height from I_1 to C_1. C_1 contains pointed cusp on anterior inner margin, in contact with I_3 outer cusp, exceeding P_2 and P_4 in height; C_1 equal to P_2 in basal area but smaller than P_4. P_2 slightly smaller than P_4 in height, and the basal and crown area of P_2 approximately 2/3 that of P_4. In lateral view, trigonids of M_1, M_2, and M_3, metaconid, and paraconid approximately 2/3 as high as protoconid

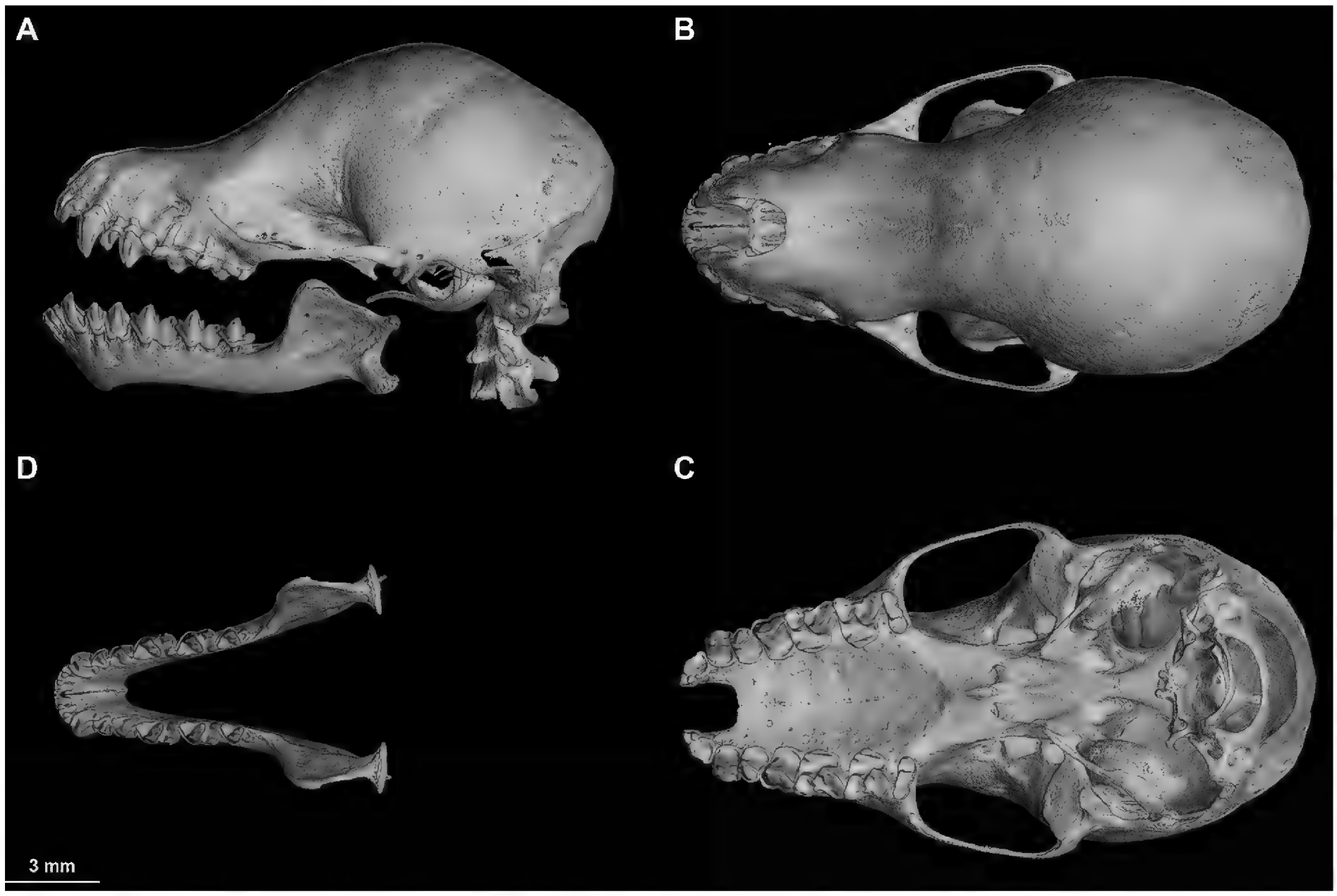

Figure 7. Micro-CT reconstruction of the skull of *Murina medogensis* sp. nov. holotype, XZ2024038. **A.** Lateral view; **B.** Dorsal view; **C.** Ventral view; **D.** Frontal view of mandible.

in height. Talonids of M_1 and M_2 are slightly half the size of trigonids; entoconids and hypoconids distinctly separated from trigonids, lower than metaconid and paraconid. M_1 and M_2 are nyctalodont types, with well-developed entoconids. M_3 reduced, talonid approximately 1/3 as long as trigonid, paraconid, protoconid, and metaconid complete and well developed.

Morphological comparisons with congeneric species. Based on its dentition, I^2 is situated laterally anterior to I^3, and I^2 is partially visible in the lateral view, and crown area of P^2 larger than 2/3 that of P^4, *Murina medogensis* sp. nov. belongs to the "*cyclotis*-type" a character that distinguishes 30 species belonging to the "*suilla*-type", I^2 is anterior to I^3, I^2 is clearly visible in the lateral view, and the crown area of P^2 is half or less than that of P^4, including *M. rubella*, *M. aurata*, *M. balaensis*, *M. beelzebub*, *M. bicolor*, *M. chrysochaetes*, *M. eleryi*, *M. fanjingshanensis*, *M. feae*, *M. fusca*, *M. gracilis*, *M. harpioloides*, *M. hilgendorfi*, *M. hkakaboraziensis*, *M. jaintiana*, *M. jinchui*, *M. kontumensis*, *M. leucogaster*, *M. liboensis*, *M. lorelieae*, *M. rongjiangensis*, *M. ryukyuana*, *M. shuipuensis*, *M. suilla*, *M. tenebrosa*, *M. tubinaris*, *M. ussuriensis*, *M. walstoni*, *M. yuanyang*, and *M. yushuensis*. Detailed morphological differences between the new species and congeners are listed in Suppl. material 5 and illustrated in Suppl. material 1: fig. S3.

Murina medogensis sp. nov. can be distinguished from *Murina beibengensis* sp. nov. by dorsal fur dark grayish overall (vs. orangish-yellow), forearm and wrists without covered sparse hairs (vs. covered with sparse hairs), lambdoid crest well developed (vs. absent), C^1 slightly less than P^4 in height (vs. C^1 taller than P^4), P_2 slightly less than P_4 in height (vs. P_2 equal to P_4), and mandibular foramina clearly visible, situated below P_4 (vs. situated below P_2).

Within the "*cyclotis*-type", *Murina beibengensis* sp. nov. different from *M. aenea*, *M. fionae*, *M. harrisoni*, *M. huttoni*, and *M. pluvialis* by the forearm length 29.75–31.24 mm (vs. forearm length over 34 mm). By dorsal hairs dark grayish, *Murina medogensis* sp. nov. can be further distinguished from *M. aenea* (vs. dark brown), *M. fionae* (vs. orange), *M. harrisoni* (vs. orangish brown), *M. huttoni* (vs. rusty brown), and *M. pluvialis* (vs. reddish brown).

Murina beibengensis sp. nov. different from *M. annamitica*, *M. cyclotis*, *M. guilleni*, *M. peninsularis*, and *M. recondita* by the sagittal crest absence (vs. presence) and dorsal hairs dark grayish (vs. orangish brown or yellowish brown). *Murina beibengensis* sp. nov. different from *M. puta* by the forearm length 29.75–31.24 mm (vs. 33.0–39.0 mm), dorsal fur (bicolored, with dark grey at the base and gray-brown tips vs. tricolored, with black at the base, tan in the middle, and reddish tips), and ventral fur silvery-gray (vs. paler). *Murina beibengensis* sp. nov. different from *M. rozendaali* by dorsal fur dark grayish (vs. shiny yellowish brown), ventral fur silvery-gray (vs. yellowish white), mesostyles of M^1 and M^2 reduced (vs. well-developed).

Table 3. External and craniodental measurements (in mm) of *M. medogensis* sp. nov. and three closely related species. NA indicates that the data is not available.

Species	*M. medogensis* sp. nov.		*M. jaintiana* (Ruedi et al. 2012)		*M. feae* (Son et al. 2015)		*M. tubinaris* (Csorba et al. 2011)
	XZ2024038 (Male)	XZ2024006 (Female)	Holotype (Male)	Range (n = 5)	Male	Female	Range
BW	4.20	4.20		NA	3.5–5.3	3.9–4.4	NA
HB	38.46	37.68	40.00	NA	33.7–43.0	32.8–43.5	NA
TL	36.37	34.54	33.00	NA	31.4–39.5	30.0–41.6	NA
EL	11.89	14.06	13.90	NA	11.5–14.3	11.0–15.0	NA
EW	6.79	6.50	NA	NA	NA	NA	NA
TRL	6.19	7.70	6.30	NA	NA	NA	NA
TRW	1.94	2.07	NA	NA	NA	NA	NA
HFL	6.94	8.52	6.80	NA	6.0–8.4	6.1–8.0	NA
FL	29.75	31.24	29.10	29.10–31.10	27.5–33.4	28.1–34.3	31.00–32.94
TIB	15.47	17.45	17.10	NA	15.7–18.1	15.6–17.8	NA
GTL	15.01	18.74	NA	14.75–15.25	14.91–16.30	15.13–16.11	14.92–15.70
CCL	14.09	16.37	NA	13.36–13.61	NA	NA	13.08–13.89
BCW	7.55	9.09	NA	NA	NA	NA	7.01–7.30
BCH	6.71	7.54	NA	5.96–6.17	NA	NA	5.55–5.86
ZYW	8.74	10.85	NA	8.26–8.68	8.50–8.90	8.9	8.07–8.66
MAW	7.11	9.32	NA	7.23–7.43	7.30–7.80	7.5	7.27–7.51
IOW	4.39	5.49	NA	4.02–4.36	NA	NA	4.28–4.51
CM^3L	4.82	7.54	NA	4.81–5.09	5.00–5.30	5.1	4.88–5.19
C^1C^1W	3.61	4.85	NA	3.52–3.74	3.70–4.00	3.9–4.4	3.59–3.78
M^3M^3W	5.07	6.72	NA	5.04–5.20	NA	NA	4.97–5.32
RCM	0.712	0.72	NA	NA	NA	NA	NA
CM_3L	5.86	7.25	NA	5.18–5.46	4.62–5.25	4.89–5.47	5.37–5.69
ML	9.1	12.54	NA	9.85–10.28	9.63–10.64	9.80–10.86	10.07–10.62
MDL	10.21	13.23	NA	NA	NA	NA	NA
CPH	3.42	2.97	NA	3.20–3.40	NA	NA	3.04–3.30

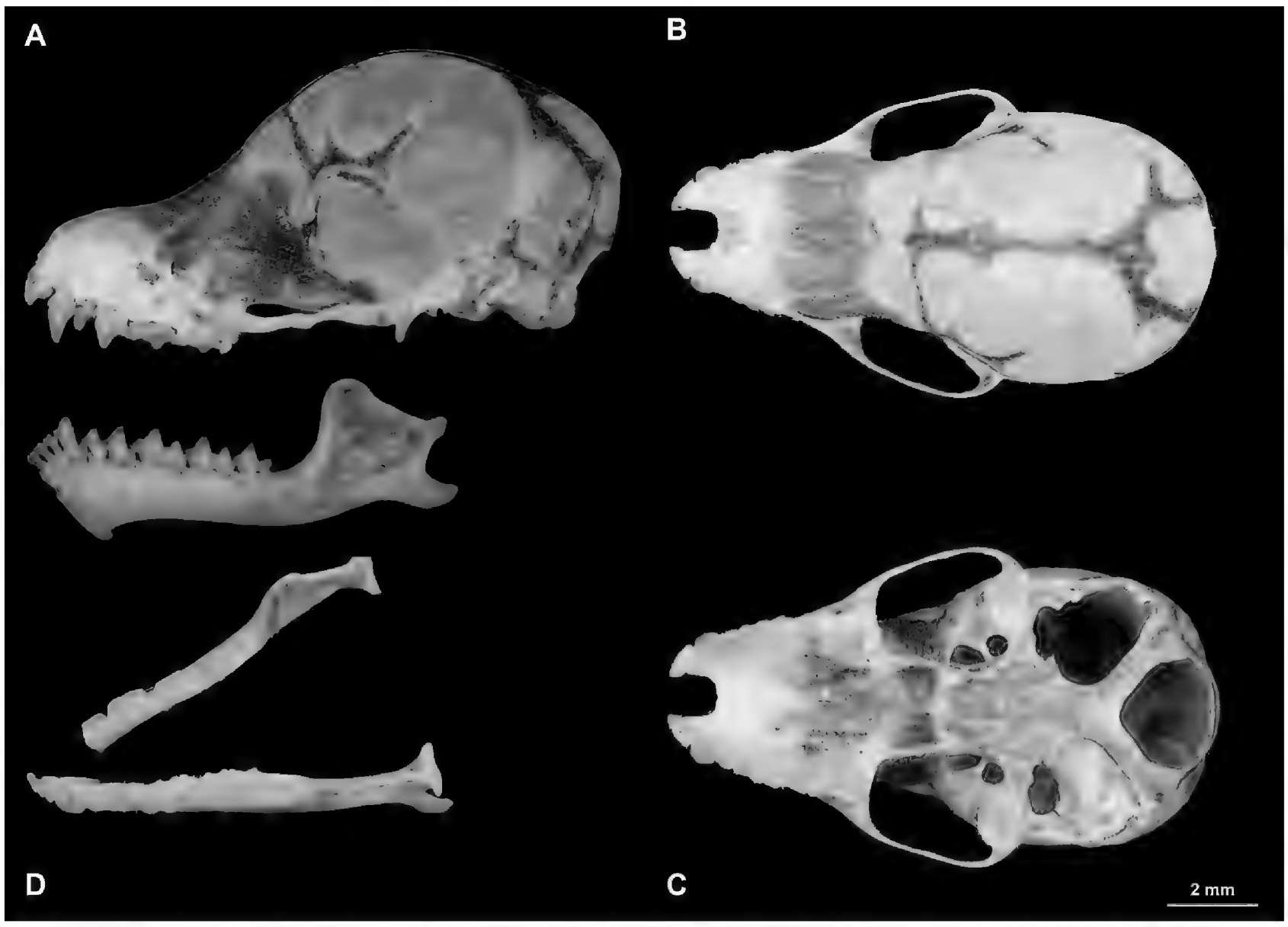

Figure 8. Skull and dentition of the *Murina medogensis* sp. nov. paratype, XZ2024006. **A.** Lateral view; **B.** Dorsal view; **C.** Ventral view; **D.** Frontal view of mandible.

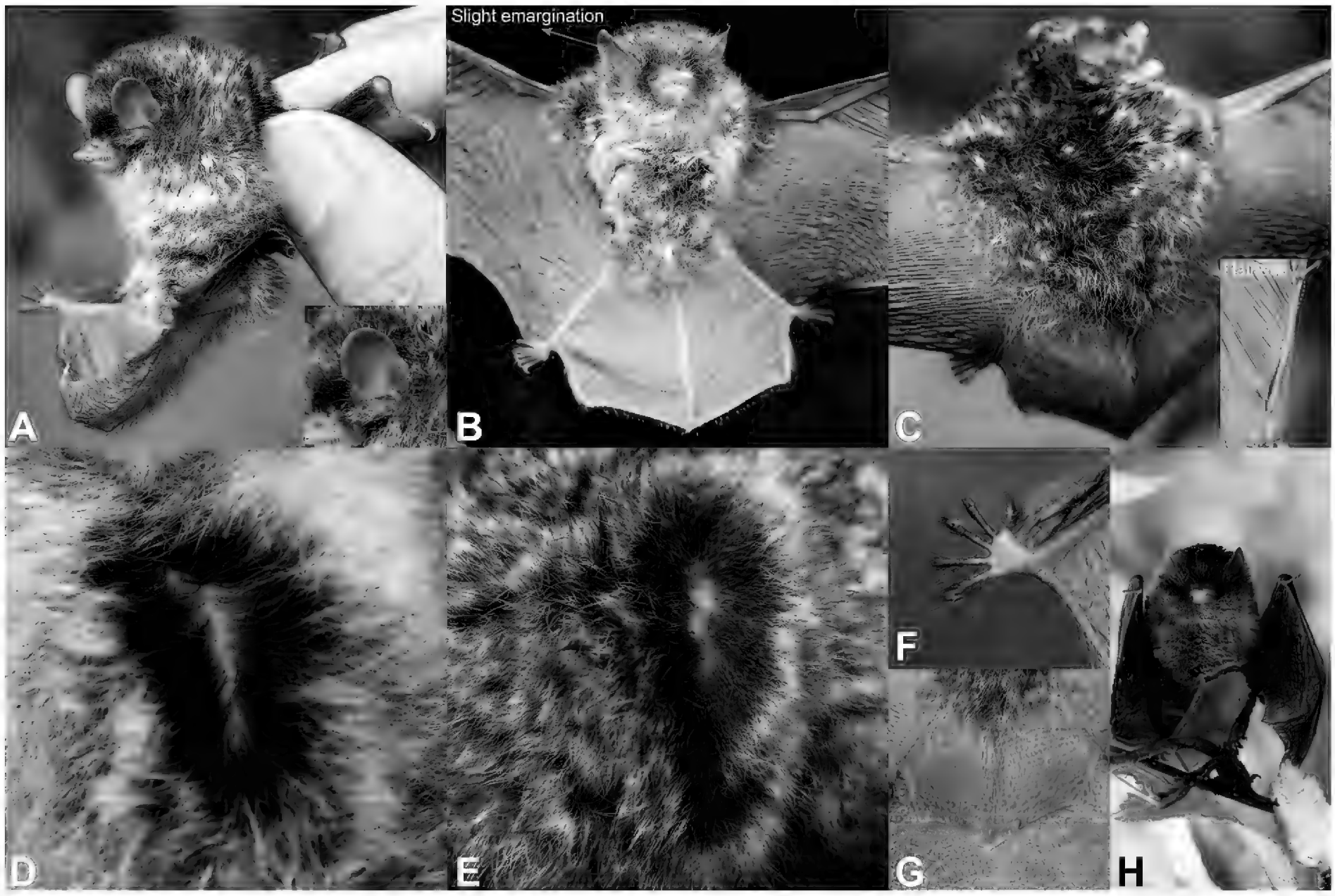

Figure 9. External morphological characteristics of *Murina medogensis* sp. nov. in living paratype, XZ2024006. **A.** Lateral view; **B.** Ventral view; **C.** Dorsal view of the body and uropatagium; **D.** Ventral hairs; **E.** Dorsal hairs; **F.** Hindfoot ventral view; **G.** Hindfoot dorsal view.

Murina medogensis sp. nov. is morphologically similar to *M. jaintiana* but can be distinctly distinguished from it by combining the following morphological characters: dorsal fur bicolored, dark grey at the base, gradually transitioning to gray-brown/white tips from 2/3 from base (vs. dorsal fur has three distinct bands: basal half dark grey, almost black, middle part dirty white, distal end brownish-grey), I^2 equal to I^3 in height (vs. I^2 smaller than I^3), C^1 slightly less than P^4 in height (vs. C^1 taller than P^4), and without distinct prominence at frontal aspect of skull (vs. with distinct prominence at frontal) (Ruedi et al. 2012).

For *M. florium* not assigned to "*suilla*-type" and "*cyclotis*-type", can be distinguished by the combination of the following morphological characters: dorsal fur dark grayish overall (vs. gray-brown to orange rufous brown), absence of notch at the posterior margin of the ear (vs. distinct notch on posterior margin), and P^2 less than P^4 in height (vs. P^2 equal to P^4).

Habitat and ecology. Currently, this new species is known only from Medog County, Nyingchi City, in the Tibet Autonomous Region, China, where two specimens were captured using a harp-shaped trap in broad-leaved evergreen forests near Medog Town, Medog County, on 16 August 2024, at two locations approximately 8 km apart. The type locality exhibits a subtropical climate, characterized by a mean annual temperature of 16 °C and mean annual precipitation ranging from 2500 to 3900 mm. The area is also surrounded by various cash crops, such as tea and banana plants. Additionally, species such as *Harpiola isodon*, *Sphaerias blanfordi*, *Myotis* sp., and *Kerivoula kachinensis* were also captured in the same region.

Murina milinensis Luo, Mao & Zhou, sp. nov.

https://zoobank.org/1A914DA7-A0EF-4301-8798-0FCDF7456399

Figs 10–12, Table 4, Suppl. material 2

Holotype. • Adult male, field number XZ2023010 (Figs 10, 11), collected by Ming-Le Mao, Chang-Ting Lan, Zi-Fa Zhao, and Zhong-Lian Wang on 14 August 2023, from Nanyi Lhoba Township, Milin County, Nyingchi City, Xizang Autonomous Region, China (29.1598922°N, 94.20712670°E; ca. 3020 m. a.s.l.; Fig. 1).

Paratypes. • Eight specimens from the same locality as the holotype. Five males, field numbers XZ2024066, XZ2024065, XZ2024067, XZ2024074, and XZ2024075. Three females, field numbers XZ202384, XZ2024072, and XZ2024076. Female XZ2024102 is from Zari Township, Longzi County, Shannan City, Xizang Autonomous Region, China (28.68318987°N, 93.34190369°E; ca. 3450 m).

Measurements (in mm) and body weight (in g) of the holotype. HB: 34.68, EL: 12.74, EW: 7.89, TRL: 7.81, TRW: 5.35, HFL: 5.31, FL: 30.02, TIB: 12.75,

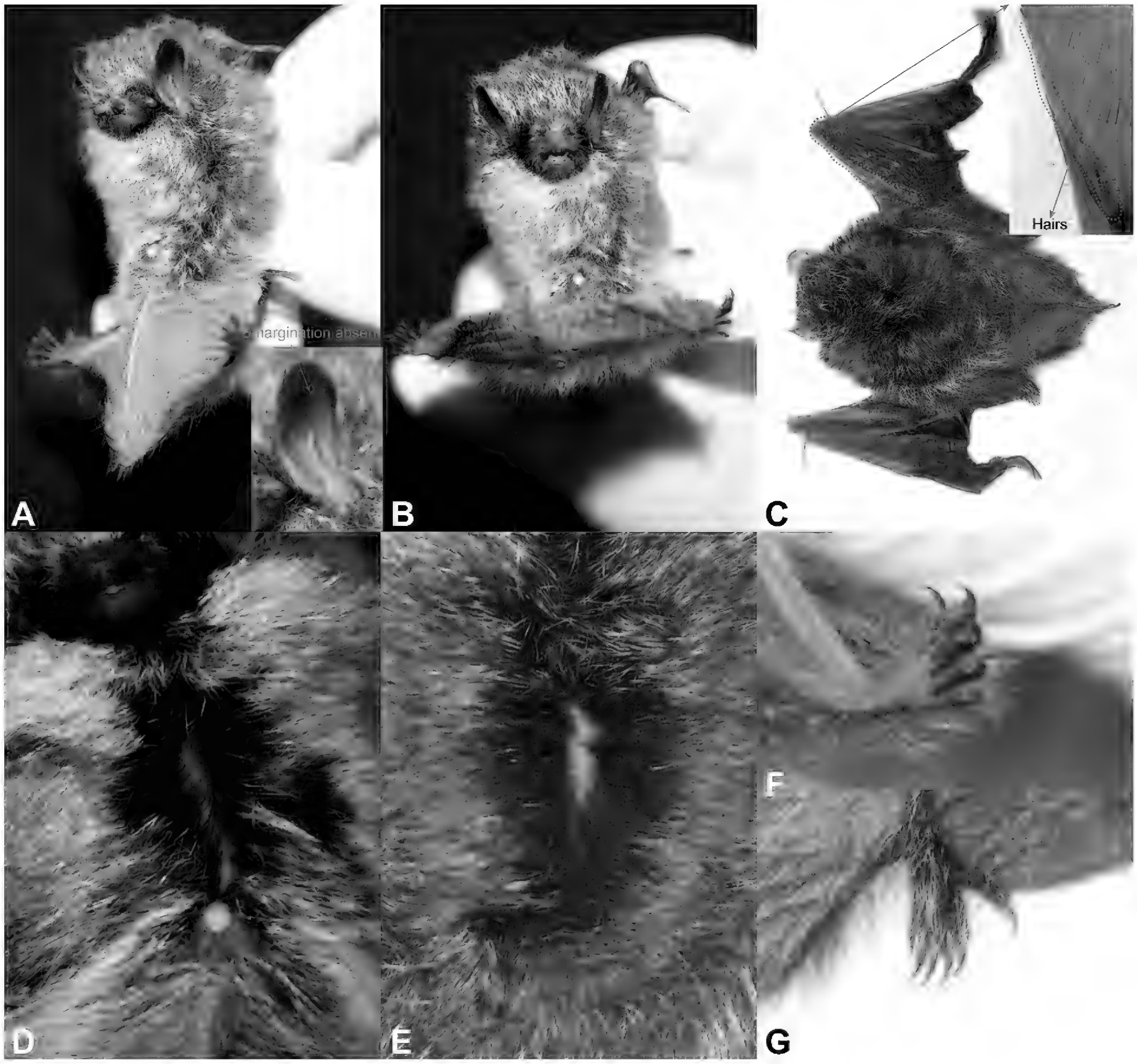

Figure 10. External morphological characteristics of *Murina milinensis* sp. nov. in living holotype, XZ2023010. **A.** Lateral view; **B.** Ventral view; **C.** Dorsal view of the body and uropatagium; **D.** Ventral hairs; **E.** Dorsal hairs; **F.** Hindfoot ventral view; **G.** Hindfoot dorsal view. These photographs were acquired under incandescent lighting conditions using a Canon EOS 6D Mark II camera ISO: 6400; focal length: 105 mm at approximately 22:41 on 5 August 2023.

GTL: 14.07, CCL: 12.01, BCW: 7.03, BCH: 6.49, ZYW: 8.07, MAW: 6.68, IOW: 4.40, CM^3L: 4.44, C^1C^1W: 2.21, M^3M^3W: 4.97, RCM: 0.44, CM_3L: 4.53, ML: 9.06, MDL: 9.46, CPH: 3.20; BW: 3.36.

Etymology. The specific epithet *milinensis* refers to the type locality of the new species: Nanyi Lhoba Township, Milin County, Nyingchi City, Xizang Autonomous Region, China. We propose the common English name "Milin Tube-nosed Bat" and the Chinese name "Mǐ Lín Guǎn Bí Fú (米林管鼻蝠)".

Diagnosis. *Murina milinensis* sp. nov. can be distinguished from all of the other congeners by the following combination of characters: (1) small-size *Murina*, FL 28.84–34.01 mm, GTL 14.07–14.27 mm; (2) dorsal fur brown-gold overall, black at the base, gradually transitioning to brown-gold tips 2/3 from the base; (3) ventral fur pale overall, dark black at the base, with grayish white at the tips; (4) ears narrow and oval, without smoothly convex anterior margins, no notch on posterior margins; (5) forearm and wrists covered with sparse hairs; (6) wing attachment point located at 1/3 from base of claw to base of toe; (7) sagittal crest absent, lambdoid crest present and poorly developed; (8) I^2 is situated anterior to I^3 and clearly visible in the lateral view, I^2 equal to I^3 in height; (9) mesostyles of M^1 and M^2 are slightly reduced; (10) C^1 less than P^4 in height, crown is about 2/3 of P^4; (11) P^2 approximately half of P^4 in height, crown area of P^2 larger than 2/3 that of P^4; (12) C_1 equal to P_4 in height and crown area; (13) mandibular foramina clearly visible, situated below anterior margin of P_4.

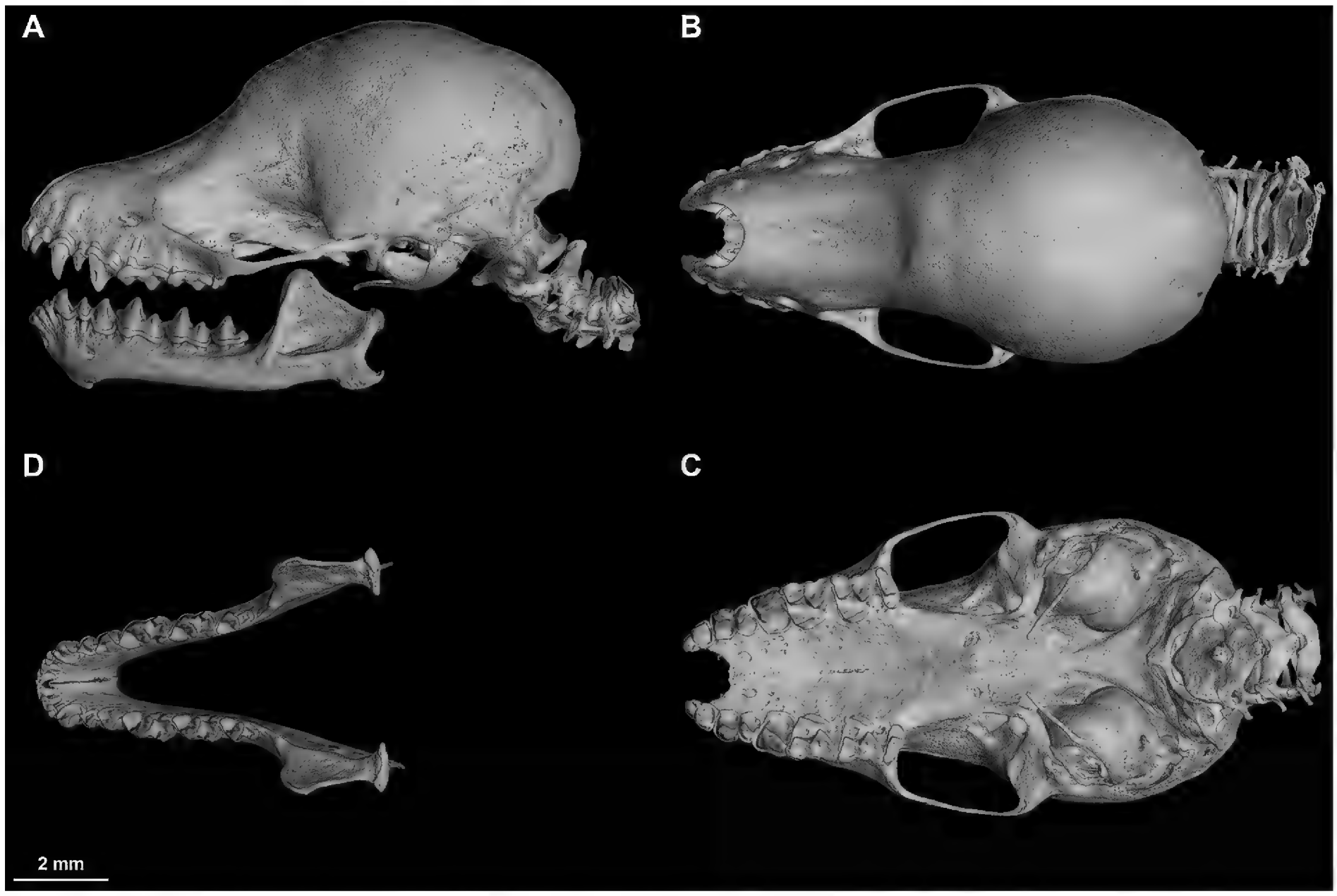

Figure 11. Micro-CT graph of the skull of *Murina milinensis* sp. nov. paratype, XZ2024066. **A.** Lateral view; **B.** Dorsal view; **C.** Ventral view; **D.** Frontal view of mandible.

Description. Morphometric data of *Murina milinensis* sp. nov. are provided in Table 4 and Suppl. material 2. Small-size *Murina*, HB 29.23–39.29 mm, FL 28.84–34.01 mm, EL 12.48–14.58 mm, HFL 5.31–9.18 mm, and BW 3.15–7.50 g. Nostrils tubular, open sideways, and slightly longer. Ears small, short, and narrow, oval, blunt at tips, with smoothly convex anterior margins, not notched on posterior margin. Tragus short, narrow, and tapering toward pointed tip, with slightly convex anterior margin, concave posterior margin, and basal notch, and it curves outwards slightly, about half as long as ear. Body covered with thick and fluffy hair. Dorsal hairs brown-gold overall (bicolored, black at the base, gradually transitioning to brown-gold tips from 2/3 from base). Dorsal hairs extend onto bases of wings, uropatagium, thumbs, forearm, wrist, tibia, and feet, with slight-developed fringe of hairs around margin of uropatagium. Densely furred anterior 1/3 of the dorsal uropatagium, posterior 2/3 covered with sparse hairs. Ventral hairs are pale overall, bicolored, bicolored, dark black at the base and grayish white at the tips. Dark flesh-purple around the eyes, muzzle, and lower forehead, and the face is hairy except for the long, protuberant nostrils that are naked. TL 24.51–30.32 mm, slightly shorter than head-body length, tip of the tail extending significantly past the rear edge of the uropatagium, tip distinctly free. Plagiopatagium attachment point located at 1/3 from base of claw to base of toe, near base of claw (Fig. 10F).

Skull robust, nearly oval, relatively small, GTL 14.07–14.27 mm. Rostrum long, deep, gradually ascending to forehead; prominent median depression present. Sagittal crest absent, lambdoid crest present, poorly developed. In dorsal view, braincase nearly domed; zygomatic arches weak and slender, gradually widening posteriorly, widest at the base of the zygomatic arches; posterior margin of skull slightly protruding; middle from snout to frontal region distinctly concave downward. In lateral view, skull slightly elongated, with elongated oval braincase; height gradually rising from snout to parietal, with slightly increasing slope from snout to frontal and decreasing slope from frontal to parietal; slight depression between snout and frontal, with slight distinct prominence at frontal; zygomatic arches gradually rising from anterior to posterior. In ventral view, palatine wide and nearly flat, ending at posterior margin of C^1; basisphenoid pits slightly shallowly tadpole-shaped, extending posteriorly to anterior half of cochlea. Mandible length 8.77–9.42 mm, inverted L-shaped in lateral view. Line between coronoid process and condyle nearly flat; distinct inward depression between condyle and angle; angle short and wide; mandibular foramina clearly visible, situated below anterior margin of P_4.

Dental morphology: Dental formula is I2/3, C1/1, P2/2, M3/3=34 (Figs 11, 12). In the maxilla, I^2 is situated anterior to I^3, and I^2 clearly visible laterally; crown area of P^2 approximately 1/3 that of P^4 and slightly

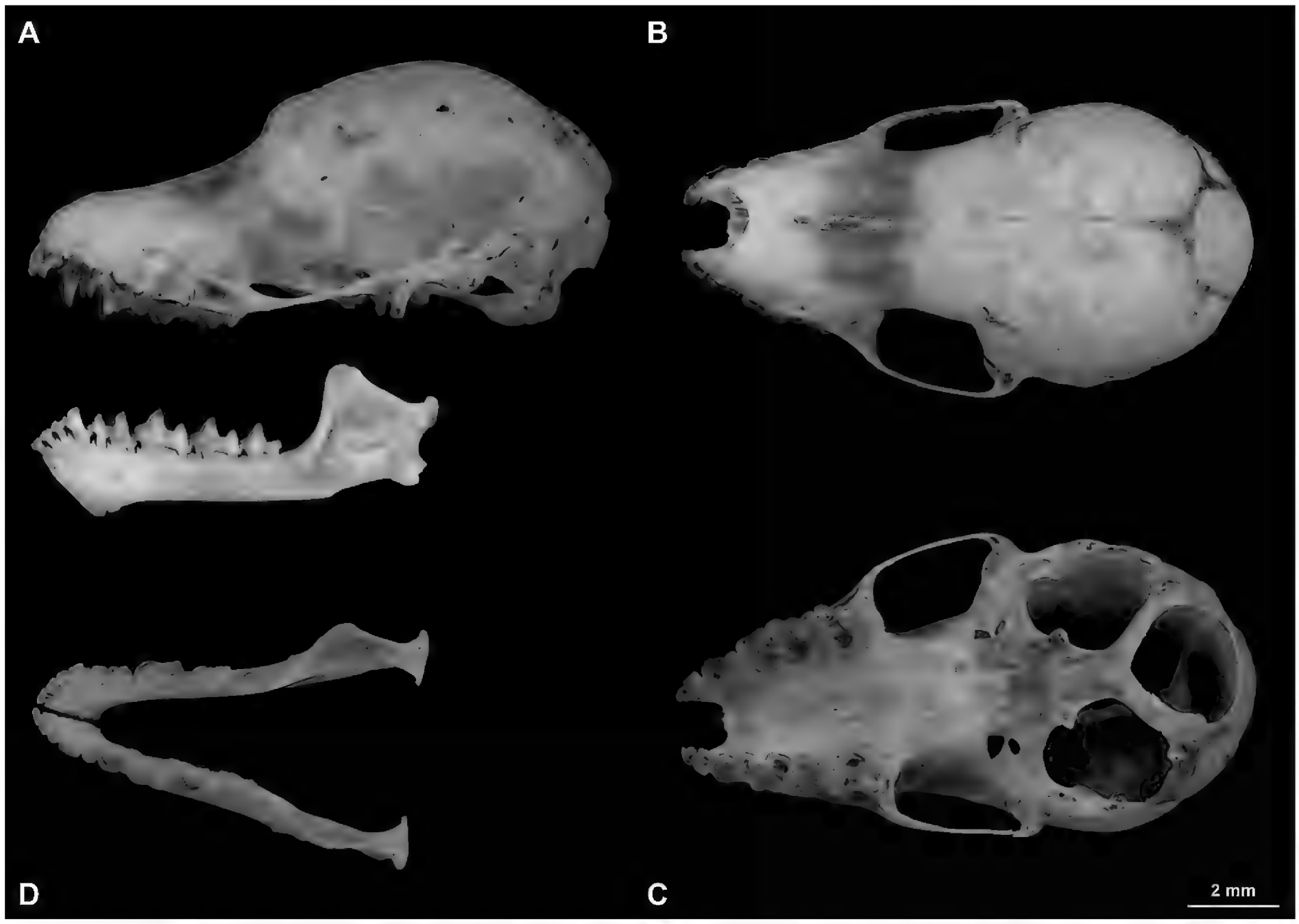

Figure 12. Skull and dentition of the *Murina milinensis* sp. nov. holotype, XZ2023010. **A.** Lateral view; **B.** Dorsal view; **C.** Ventral view; **D.** Frontal view of mandible.

smaller than C^1. Based on these characters, the species belongs to the "*suilla*-type". Maxillary dentition converges slightly anteriorly (RCM = 0.44–0.70). I^2 and I^3 bicuspid, smaller secondary cusp situated posterior to primary cusp; I^2 almost equal to I^3 in height, crown area of I^2 half that of I^3; distinct gap between posterior surface of I^3 and C^1, not in contact, about half of height of C^1. C^1 less than P^4 in height, slightly elongated and lacking secondary cusps, crown area half that of P^4; P^2 slightly smaller, delicate and pointed, about half as high as P^4 and 2/3 as high as C^1, and crown area of P^2 is half that of P^4 and slightly smaller than C^1. Mesostyles of M^1 and M^2 are reduced, but retaining distinct cusps; paracone, protocone, metacone, and parastyle well developed. M^3 reduced, with only parastyle, paracone, and protocone. In the mandible, I_1, I_2, and I_3 smaller, tricuspid, almost equal in height and width; slight overlap of outer cusps of I_1, I_2, and I_3; with gradual increase in height from I_1 to C_1. C_1 contains pointed cusp on anterior inner margin, in contact with I_3 outer cusp. C_1 taller than P_2 and P_4 in height, with a basal area larger than P_2 but smaller than P_4. P_2 equal to P_4 in height, and the basal and crown areas are about half of P_4. In lateral view, trigonids of M_1, M_2, and M_3 clearly bicuspid, metaconid, and paraconid approximately 2/3 as high as protoconid in height. Talonid of M_1 and M_2 is slightly half the size of trigonid; entoconid and hypoconid distinctly separated from trigonid, lower than metaconid and paraconid, nearly equal to metaconid and paraconid in height. M_1 and M_2 are nyctalodont types, with well-developed entoconids. M_3 reduced, talonid approximately 1/3 as long as trigonid, paraconid, protoconid, and metaconid complete and well developed.

Morphological comparisons with congeneric species. Based on its dentition, I^2 situated anterior to I^3, and the crown area of P^2 is less than half that of P^4 and smaller than that of C^1, *Murina beibengensis* sp. nov. belongs to the "*suilla*-type", a character that distinguishes 12 species belonging to the "*cyclotis*-type," including *M. aenea*, *M. annamitica*, *M. cyclotis*, *M. fionae*, *M. guilleni*, *M. harrisoni*, *M. huttoni*, *M. peninsularis*, *M. pluvialis*, *M. puta*, *M. recondita*, and *M. rozendaali*. Detailed morphological differences between the new species and congeners are listed in Suppl. material 5 and illustrated in Suppl. material 1: fig. S3.

Murina milinensis sp. nov. can be distinguished from *Murina beibengensis* sp. nov. by dorsal fur dark grayish overall (vs. brown-gold), ventral fur black at the base (vs. dark grey at the base), sagittal crest absent (vs. well-developed), I^2 is situated laterally anterior to I^3, and I^2 is partially visible in the lateral view (vs. I^2 is anterior to I^3, I^2 is clearly visible in the lateral view), I^2 equal to I^3 in height (vs. I^2 taller than I^3), and C^1 slightly less than P^4 in height (vs. C^1 taller than P^4).

Table 4. External and craniodental measurements (in mm) of *M. milinensis* sp. nov., *M. yadongensis* sp. nov., and four closely related species. MC: *M. chrysochaetes* (Eger et al. 2011); MH: *M. harpioloides* (Kruskop and Eger 2008); MY: *M. yushuensis* (Wang et al. 2024a). NA indicates that the data is not available.

Species	*M. yadongensis* sp. nov.		*M. milinensis* sp. nov.		MC	MH	MY	*M. yuanyang* (Mou et al. 2024)		
	Male (n = 3)	Female (n = 1)	Male (n = 6)	Female (n = 4)	Holotype (male)	Holotype (male)	Holotype (male)	Holotype (male)	Male (n = 2)	Female (n = 5)
BW	5.68–7.00 (6.52 ± 0.73)	6.86	3.15–3.49 (3.37 ± 0.12)	3.35–7.50 (4.73 ± 1.88)	NA	NA	NA	4.20	3.4–3.6	3.8–4.7 (4.3 ± 0.3)
HB	28.68–35.54 (32.21 ± 3.43)	33.88	33.70–37.89 (35.78 ± 1.57)	29.23–39.29 (34.30 ± 5.60)	NA	35.00	30.44	35.05	31.37–35.94	32.11–36.34 (34.82 ± 1.52)
TL	28.32–30.46 (29.52 ± 1.09)	32.12	25.54–30.32 (28.88 ± 1.69)	24.51–28.98 (26.66 ± 2.29)	28.00	30.50	28.08	31.58	23.89–27.25	26.92–31.58 (28.39 ± 1.64)
EL	11.40–14.02 (12.85 ± 1.33)	14.2	12.48–14.58 (13.46 ± 0.82)	13.12–13.95 (13.55 ± 0.34)	11.00	12.30	11.08	12.99	12.77–13.4	12.27–14.77 (13.25 ± 0.82)
EW	6.20–7.06 (6.54 ± 0.46)	8.04	6.92–8.47 (7.70 ± 0.52)	6.76–8.58 (7.38 ± 0.84)	NA	NA	NA	NA	NA	NA
TRL	7.15–7.49 (7.37 ± 0.19)	7.81	6.59–7.82 (7.31 ± 0.51)	6.28–8.35 (7.22 ± 1.04)	NA	NA	NA	NA	NA	NA
TRW	2.14–2.15 (2.14 ± 0.01)	2.13	1.51–5.35 (2.49 ± 1.42)	1.76–2.34 (2.03 ± 0.28)	NA	NA	NA	NA	NA	NA
HFL	6.07–8.55 (7.15 ± 1.27)	7.06	5.31–8.89 (7.37 ± 1.32)	6.82–9.18 (7.94 ± 0.97)	7.00	NA	8.46	7.88	6.14–6.83	6.25–8.52 (7.66 ± 0.75)
FL	28.81–30.29 (29.60 ± 0.75)	31.84	28.84–30.43 (29.82 ± 0.60)	30.83–34.01 (32.12 ± 1.35)	26.35	29.70	31.34	29.80	NA	NA
TIB	13.57–14.27 (13.82 ± 0.39)	14.61	12.64–13.95 (13.42 ± 0.60)	13.32–14.37 (13.94 ± 0.44)	10.92	NA	15.22	13.48	12.56–13.16	12.37–13.57 (13.15 ± 0.43)
GTL	13.73–14.11 (13.92 ± 0.27)	NA	14.07–14.27 (14.17 ± 0.14)	14.16	14.05	NA	14.14	14.13	13.44–14	13.95–14.16 (14.09 ± 0.07)
CCL	12.61–12.89 (12.75 ± 0.20)	NA	12.01–13.29 (12.65 ± 0.91)	12.26	12.45	12.34	13.85	12.12	11.58–11.93	11.94–12.22 (12.10 ± 0.09)
BCW	6.36–6.70 (6.53 ± 0.24)	NA	6.81–7.03 (6.92 ± 0.16)	6.92	6.98	7.21	7.23	6.95	6.91–6.93	6.93–7.15 (7.00 ± 0.08)
BCH	5.66–6.53 (6.10 ± 0.62)	NA	6.25–6.49 (6.37 ± 0.17)	6.64	NA	5.81	6.05	6.78	6.59–6.98	6.51–6.78 (6.62 ± 0.09)
ZYW	7.76–8.72 (8.24 ± 0.68)	NA	7.63–8.07 (7.85 ± 0.31)	7.38	7.85	NA	7.94	7.73	7.41–7.52	7.44–7.81 (7.69 ± 0.13)
MAW	7.03–7.04 (7.04 ± 0.01)	NA	6.13–6.68 (6.41 ± 0.39)	6.06	7.07	7.42	6.89	7.21	7.18–7.23	7.12–7.38 (7.31 ± 0.10)
IOW	3.51–4.39 (3.95 ± 0.62)	NA	3.98–4.40 (4.19 ± 0.30)	3.82	NA	4.09	4.31	3.84	3.67–3.78	3.68–3.86 (3.79 ± 0.06)
CM^3L	4.46–5.31 (4.89 ± 0.60)	NA	4.32–4.44 (4.38 ± 0.08)	4.66	4.36	4.68	4.42	4.51	4.38–4.43	4.45–4.63 (4.53 ± 0.06)
C^1C^1W	2.19–2.45 (2.32 ± 0.18)	NA	2.21–3.32 (2.77 ± 0.78)	2.07	NA	NA	NA	3.22	3.01–3.21	3.06–3.28 (3.21 ± 0.08)
M^3M^3W	3.30–3.80 (3.55 ± 0.35)	NA	4.74–4.97 (4.86 ± 0.16)	3.38	4.36	4.88	4.83	4.74	4.59–4.61	4.62–4.74 (4.67 ± 0.04)
RCM	0.64–0.66 (0.65 ± 0.01)	NA	0.44–0.70 (0.57 ± 0.18)	0.61	0.73	0.69	0.67	0.68	NA	NA
CM_3L	4.91–5.74 (5.33 ± 0.59)	NA	4.53–5.11 (4.82 ± 0.41)	5.08	4.36	5.13	4.09	5.03	4.71–4.81	4.88–5.03 (4.93 ± 0.05)
ML	8.85–9.22 (9.04 ± 0.26)	NA	8.77–9.06 (8.92 ± 0.21)	9.42	8.42	9.31	9.08	8.41	8.09–8.15	8.34–8.69 (8.49 ± 0.13)
MDL	8.72–9.49 (9.11 ± 0.54)	NA	9.24–9.46 (9.35 ± 0.16)	9.82	8.42	NA	NA	8.76	8.21–8.43	8.51–8.91 (8.75 ± 0.13)
CPH	3.30–3.61 (3.46 ± 0.22)	NA	2.99–3.20 (3.10 ± 0.15)	3.31	3.06	3.32	2.96	2.86	2.52–2.76	2.69–2.93 (2.83 ± 0.09)

Murina milinensis sp. nov. can be distinguished from *Murina medogensis* sp. nov. by dorsal fur brown-gold (s. dark grayish), ventral fur pale (vs. silvery-gray), dorsal hairs extend onto forearm and wrist (vs. hairless forearms and wrists), I^2 is situated laterally anterior to I^3, and I^2 is partially visible in the lateral view (vs. I^2 is anterior to I^3, I^2 is clearly visible in the lateral view), and I^2 equal to I^3 in height (vs. I^2 taller than I^3).

Murina milinensis sp. nov. can be distinguished from *M. fanjingshanensis*, *M. fusca*, *M. hilgendorfi*, and

M. leucogaster by the small size, forearm length 28.84–34.01 mm, and greatest length of skull 14.07–14.27 mm (vs. forearm length over 37 mm and greatest length of skull over 16 mm in the latter).

Murina milinensis sp. nov. can be distinguished from *M. aurata* by dorsal fur brown-gold, bicolored, black at the base, gradually transitioning to brown-gold tips from 2/3 from base (vs. golden brown), from *M. balaensis* (vs. orange-reddish), from *M. eleryi* (vs. coppery brown), from *M. feae* (vs. dark grayish), from *M. jaintiana* (vs. medium gray with brownish tinge), from *M. jinchui* (vs. brownish gray), from *M. liboensis* (vs. yellowish brown), from *M. lorelieae* (vs. reddish brown), from *M. walstoni* (vs. brownish gray), from *M. walstoni* (vs. warm brown, whitish at the base, orangish brown at tips), and from *M. yuanyang* (vs. bark gold). *M. milinensis* sp. nov. can be further distinguished from *M. bicolor* by ventral fur is pale overall, bicolored, dark at the base, pale at tips (vs. uniformly yellow), from *M. rongjiangensis* (vs. bright yellowish orange), and from *M. shuipuensis* (vs. bright orange yellow).

Murina milinensis sp. nov. can be distinguished from *M. beelzebub*, *M. gracilis*, *M. harpioloides*, *M. hkakaboraziensis*, *M. kontumensis*, and *M. suilla* by the ears without smooth convex anterior margins and no notch on posterior margin (vs. with smoothly convex anterior margins, distinct notch on posterior margin); from *M. chrysochaetes*, *M. ryukyuana*, *M. tenebrosa*, *M. ussuriensis*, and *M. yushuensis* (vs. with smoothly convex anterior margins). By lambdoid crest absent and I^2 equal to I^3 in height, *Murina milinensis* sp. nov. can be further distinguished from *M. rubella* and *M. chrysochaetes* (vs. present, I^2 less than I^3); from *M. rongjiangensis* (vs. present, I^2 taller than I^3), and *M. yushuensis* (vs. present). *Murina milinensis* sp. nov. can be distinguished from *M. bicolor* by sagittal crest absent (vs. present), C^1 slightly less than P^4 in height (vs. C^1 taller than P^4), P_2 less than P_4 in height (vs. P_2 taller than P4), and C_1 taller than P_4 in height (vs. C_1 equal to P_4).

Murina milinensis sp. nov. can be distinguished from *M. tubinaris* by dorsal hairs brown-gold (vs. light gray), P_2 less than P_4 in height (vs. P_2 taller than P_4), ears without smooth convex anterior margins and no notch on posterior margin (vs. with smoothly convex anterior margins and small notch on posterior margins), and basal area of P^2 is larger than one-half that of P^4 (vs. less than one-half that of P^4).

For *M. florium* not assigned to "*suilla*-type" and "*cyclotis*-type", can be distinguished by the combination of the following morphological characters: absence of notch at the posterior margin of the ear (vs. distinct notch on posterior margin), I^2 almost equal to I^3 in height (vs. I^2 taller than I^3), and P^2 slightly less than P^4 in height and crown area (vs. equally).

Habitat and ecology. Currently, this new species is known only from two areas in the Xizang Autonomous Region, China. The type specimen was captured using a harp trap in a water channel near Nanyi Lhoba Township, Miling County, Nyingchi City, on 14 August 2023. A single additional specimen of the same species (Specimen No. XZ2023084) was also captured at the same site. The water channel was approximately 4 m wide and 3 m deep, with a shallow flow of water (approximately 25 cm deep). Dense thickets grew along both sides of the channel. Nanyi Lhoba Township, situated at an elevation of about 3020 m, experiences a plateau temperate semi-humid monsoon climate, with an average annual temperature of approximately 9.3 °C and an annual rainfall of around 600 mm. The collection site is located in a river valley, surrounded by mixed coniferous and broadleaf forests as well as agricultural land, where wheat, highland barley, and oilseed rape are the primary crops. In August of the following year, we captured seven specimens of the same species at the same site. Additionally, the presence of *Myotis* sp. was recorded in this area.

Another distribution site is located in the mixed coniferous and broadleaf forest near Zari Township, Longzi County, Shannan City, where one specimen was captured using a harp-shaped trap. This site has a plateau temperate continental monsoon climate, with an average annual temperature of 10.3 °C and annual precipitation ranging from 350 to 550 mm. The collection site is also situated in a river valley with dense vegetation. In the vicinity, we recorded *Rhinolophus* sp. and *Myotis* sp.

Murina yadongensis Mao, Zhao & Zhou, sp. nov.

https://zoobank.org/4417D227-ACC0-4FA4-96ED-9D0A87D30385

Figs 13, 14, Table 4, Suppl. material 2

Holotype. • Adult male, field number XZ2023082 (Figs 13, 14), collected by Ming-Le Mao, Qing-Qing He, and Qin Yang, on 6 August 2023, at Boluoka, Xiayadong Township, Yadong County, Shigatse City, Xizang Autonomous Region, China (27.36420685°N, 88.97613108°E; ca. 2775 m. a.s.l.; Fig. 1).

Paratypes. • Three specimens from the same locality as the holotype. Two males, field numbers XZ2023036 and XZ2023016. One female, field numbers XZ2023062. XZ2023082 and XZ2023062 have been dissected for sampling and are incomplete specimens.

Measurements (in mm) and body weight (in g) of the holotype. HB: 35.54, EL: 14.02, EW: 6.20, TRL: 7.48, TRW: 2.14, HFL: 6.07, FL: 30.29, TIB: 13.57, GTL: 13.73, CCL: 12.61, BCW: 6.36, BCH: 5.66, ZYW: 8.72, MAW: 7.04, IOW: 3.51, CM^3L: 5.31, C^1C^1W: 2.45, M^3M^3W: 3.80, RCM: 0.64, CM_3L: 5.74, ML: 9.22, MDL: 9.49, CPH: 3.61; BW: 5.68.

Etymology. The specific epithet *yadongensis* refers to the type locality of the new species: Xiayadong Township, Yadong County, Shigatse City, Xizang Autonomous Region, China. We propose the common English name "Yadong Tube-nosed Bat" and the Chinese name "Yà Dōng Guǎn Bí Fú (亚东管鼻蝠)".

Diagnosis. *Murina yadongensis* sp. nov. can be distinguished from all of the other congeners by the following

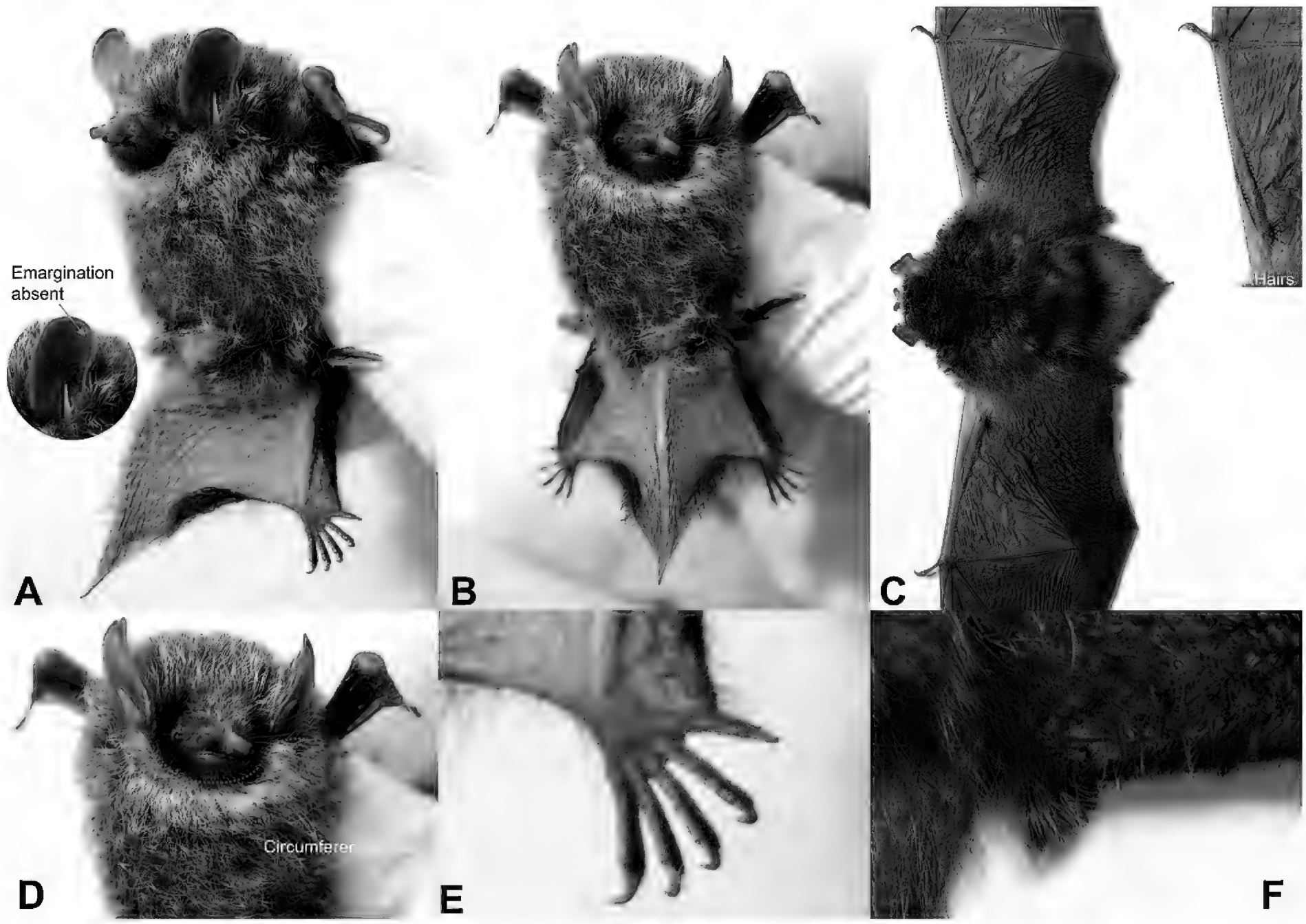

Figure 13. External morphological characteristics of the *Murina yadongensis* sp. nov. in living holotype XZ2023082. **A.** Lateral view; **B.** Ventral view; **C.** Dorsal view of the body and uropatagium; **D.** Ventral hairs; **E.** Dorsal hairs; **F.** Hindfoot ventral view; **G.** Hindfoot dorsal view.

combination of characters: (1) small-size *Murina*, FL 28.81–31.84 mm, GTL 13.73–14.11 mm; (2) dorsal fur brown-gold, black at the base, gradually transitioning to brown-gold tips 2/3 from base; (3) ventral fur grayish brown, black at the base, gray-white at tips; (4) ears narrow and oval, without smoothly convex anterior margins, no notch on posterior margins; (5) forearm and wrists covered with sparse hairs; (6) wing attachment point located at 1/3 from base of claw to base of toe; (7) an off-white circumferential band around the neck; (8) sagittal crest absent, lambdoid crest present, poorly developed; (9) I^2 is situated anterior to I^3 and clearly visible in lateral view, I^2 equal to I^3 in height; (10) mesostyles of M^1 and M^2 are slightly reduced; (11) C^1 taller than P^4, crown is about 2/3 of P^4; (12) P_2 exceeded 2/3 of P_4 in height, and the crown area is about 2/3 of P_4; (13) C_1 equal to P_4 in height and crown area. and crown area of P^2 larger than 2/3 that of P^4.

Description. Morphometric data of *Murina yadongensis* sp. nov. are provided in Table 4 and Suppl. material 2. Small-size *Murina*, HB 28.68–35.54 mm, FL 28.81–31.84 mm, EL 11.40–14.20 mm, HFL 6.07–8.55 mm, and BW 5.68–7.00 g. Nostrils tubular, open sideways, and slightly longer. Ears small, short, and narrow, oval, blunt at tips, without smoothly convex anterior margins, not notched on posterior margin. Tragus short, narrow, and tapering toward pointed tip, with slightly convex anterior margin, concave posterior margin, and basal notch, and it curves outwards slightly, about half as long as ear. Body covered with thick and fluffy hair. Dorsal hairs brown-gold (bicolored, black at the base, gradually transitioning to brown-gold tips from 2/3 from base). Dorsal hairs extend onto bases of wings, uropatagium, thumbs, forearm, wrist, tibia, and feet, with slight-developed fringe of hairs around margin of uropatagium. Densely furred anterior 1/3 of the dorsal uropatagium, posterior 2/3 covered with sparse hairs. Ventral hairs grayish brown overall, bicolored, black at the base, gray-white at tips. An off-white circumferential band around the neck. Dark flesh-purple around the eyes, muzzle, and lower forehead, and the face is hairy except for the long, protuberant nostrils that are naked. TL 28.32–32.12 mm, slightly shorter than head-body length, tip of the tail extending significantly past the rear edge of the uropatagium, tip distinctly free. Plagiopatagium attachment point located at 1/3 from base of claw to base of toe, near base of claw (Fig. 13E, F).

Skull robust, nearly oval, relatively small, GTL 13.73–14.11 mm. Rostrum long, deep, gradually ascending to forehead; prominent median depression present. Sagittal and lambdoid crests absent. In dorsal view, braincase domed; zygomatic arches weak and slender, gradually widening posteriorly, widest at the base of the zygomatic arches; posterior margin of skull slightly protruding; mid-

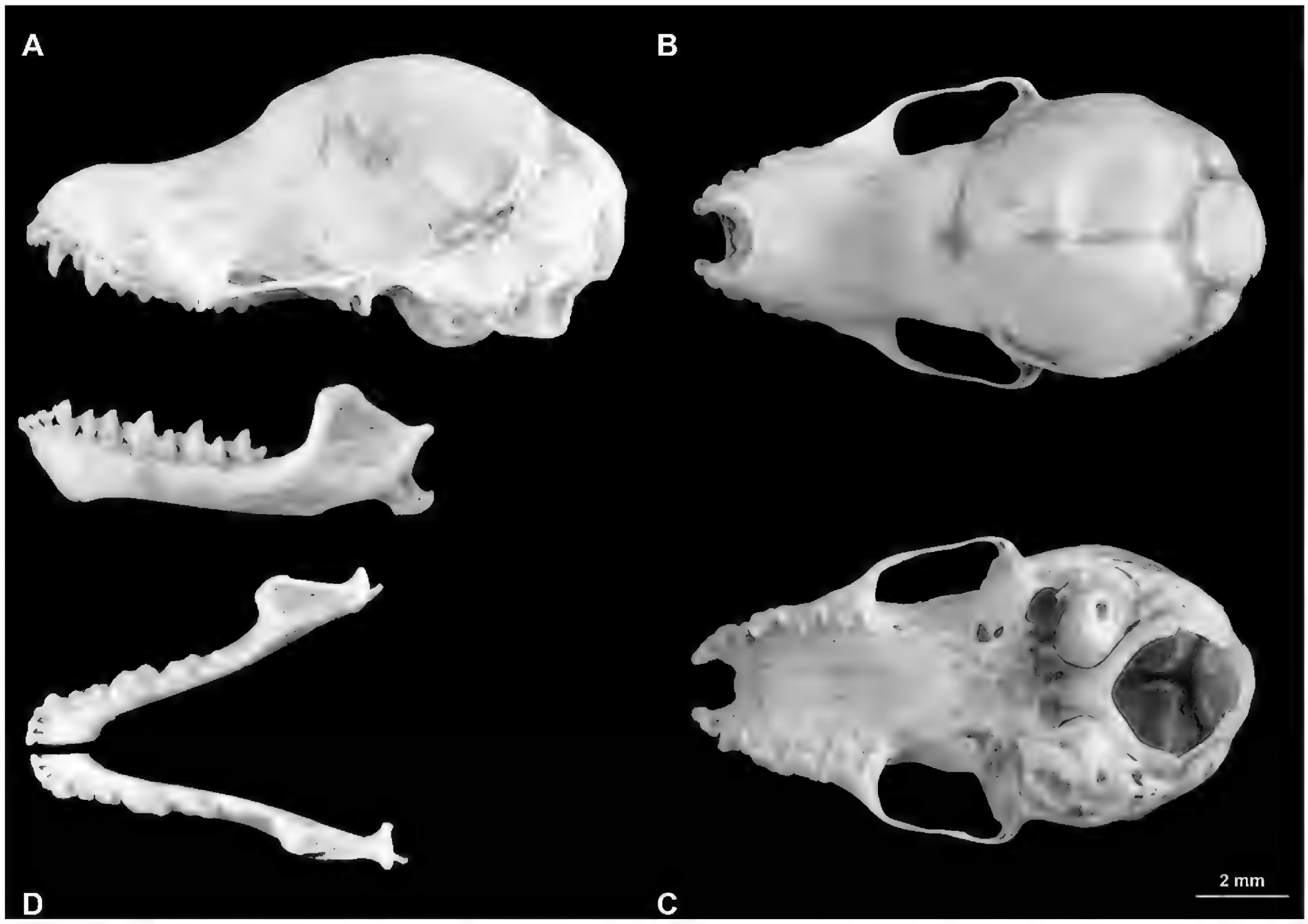

Figure 14. Skull and dentition of the *Murina yadongensis* sp. nov. holotype, XZ2023082. **A.** Lateral view; **B.** Dorsal view; **C.** Ventral view; **D.** Frontal view of mandible.

dle from snout to frontal region distinctly concave downward. In lateral view, skull slightly elongated, with elongated oval braincase; height gradually rising from snout to parietal, with slightly increasing slope from snout to frontal and decreasing slope from frontal to parietal; slight depression between snout and frontal, with slight distinct prominence at frontal; zygomatic arches gradually rising from anterior to posterior. In ventral view, palatine wide and nearly flat, ending at posterior margin of C^1; basisphenoid pits slightly shallowly tadpole-shaped, extending posteriorly to anterior half of cochlea. Mandible length 8.85–9.22 mm, inverted L-shaped in lateral view. Line between coronoid process and condyle nearly flat; distinct inward depression between condyle and angle; angle short and wide; mandibular foramina clearly visible, situated below anterior margin of P_4.

Dental morphology: Dental formula is I2/3, C1/1, P2/2, M3/3=34 (Fig. 14). In the maxilla, I^2 is situated anterior to I^3, and I^2 clearly visible laterally; crown area of P^2 approximately half that of P^4 and slightly smaller than C^1. Based on these characters, the species belongs to the "*suilla*-type". Maxillary dentition converges slightly anteriorly (RCM = 0.64–0.66). I^2 and I^3 bicuspid, smaller secondary cusp situated posterior to primary cusp; I^2 almost equal to I^3 in height, with crown area approximately half that of I^3; distinct gap between posterior surface of I^3 and C^1, not in contact, about half of height of C^1. C^1 smaller than P^4 in height, slightly elongated and lacking secondary cusps, crown area 2/3 that of P^4; P^2 slightly smaller, delicate and pointed, about half as tall as P^4 and C^1, with crown area of P^2 is half that of P^4 and slightly smaller than C^1. Mesostyles of M^1 and M^2 are reduced, but retaining distinct cusps; paracone, protocone, metacone, and parastyle well developed. M^3 reduced, with only parastyle, paracone, and protocone. In the mandible, I_1, I_2, and I_3 smaller, tricuspid, almost equal in height and width; overlap of outer cusps of I_1, I_2, and I_3; with rapid increase in height from I_3 to C_1. C_1 without pointed cusp on anterior inner margin, not in contact with I_3 outer cusp. C_1 almost equal to P_4 in height and basal area, about twice as much as P_2. P_2 exceeded 4/5 of P_4 in height, and the basal and crown areas are about 2/3 of P_4. In lateral view, trigonids of M_1, M_2, and M_3, metaconidhe slightly equal to protoconid in height, paraconid about 1/3 of protoconid. Talonid of M_1 and M_2 almost the same size as trigonid; entoconid and hypoconid distinctly separated from trigonid, lower than metaconid and paraconid, nearly equal to metaconid and paraconid in height. M_1 and M_2 are nyctalodont types, with well-developed entoconids. M_3 reduced, talonid approximately 1/3 as long as trigonid, paraconid, protoconid, and metaconid complete and well developed.

Morphological comparisons with congeneric species. Based on its dentition, I^2 situated anterior to I^3, and the crown area of P^2 is less than half that of P^4 and smaller than that

of C^1, *Murina beibengensis* sp. nov. belongs to the "*suilla*-type," a character that distinguishes 12 species belonging to the "*cyclotis*-type," including *M. aenea*, *M. annamitica*, *M. cyclotis*, *M. fionae*, *M. guilleni*, *M. harrisoni*, *M. huttoni*, *M. peninsularis*, *M. pluvialis*, *M. puta*, *M. recondita*, and *M. rozendaali*. Detailed morphological differences between the new species and congeners are listed in Suppl. material 5 and illustrated in Suppl. material 1: fig. S3.

Murina yadongensis sp. nov. can be distinguished from *Murina beibengensis* sp. nov. by dorsal fur brown-gold (vs. brown-gold), sagittal crest absent (vs. well-developed), I^2 is situated laterally anterior to I^3, and I^2 is partially visible in the lateral view (vs. I^2 is anterior to I^3, I^2 is clearly visible in the lateral view), I^2 almost equal to I^3 in height (vs. I^2 taller than I^3), and C^1 taller than P^4 in height (vs. C^1 almost equal to P^4).

Murina yadongensis sp. nov. can be distinguished from *Murina medogensis* sp. nov. by brown-gold dorsal fur (vs. dark grayish), dorsal hairs extend onto forearm and wrist (vs. hairless forearms and wrists), I^2 is situated laterally anterior to I^3, and I^2 is partially visible in the lateral view (vs. I^2 is anterior to I^3, I^2 is clearly visible in the lateral view), I^2 almost equal to I^3 in height (vs. I^2 higher than I^3), C^1 taller than P^4 (vs. C^1 almost equal to P^4), and an off-white circumferential band around the neck (vs. lacking); from *Murina milinensis* sp. nov. by lambdoid crest absent (vs. poorly developed), C^1 taller than P^4 (vs. C^1 lower than P^4), C_1 taller than P_4 (vs. C_1 equal to P_4), and an off-white circumferential band around the neck (vs. lacking).

Murina yadongensis sp. nov. can be distinguished from *M. bicolor*, *M. fanjingshanensis*, *M. fusca*, *M. hilgendorfi*, *M. jinchui*, *M. leucogaster*, and *M. ryukyuana* by the small size, forearm length 28.81–31.84 mm (vs. forearm length over 35 mm).

Murina yadongensis sp. nov. can be distinguished from *M. aurata*, *M. balaensis*, *M. beelzebub*, *M. bicolor*, *M. chrysochaetes*, *M. eleryi*, *M. fanjingshanensis*, *M. feae*, *M. florium*, *M. hilgendorfi*, *M. hkakaboraziensis*, *M. jaintiana*, *M. jinchui*, *M. leucogaster*, *M. liboensis*, *M. lorelieae*, *M. rongjiangensis*, *M. ryukyuana*, *M. shuipuensis*, *M. suilla*, *M. tenebrosa*, *M. tubinaris*, *M. ussuriensis*, *M. walstoni*, *M. yuanyang*, and *M. yushuensis* by an off-white circumferential band around the neck (vs. absent). By dorsal fur brown-gold (bicolored, black at the base, gradually transitioning to brown-gold tips from 2/3 from base), *Murina yadongensis* sp. nov. can be further distinguished from *M. aurata* (vs. golden brown), *M. balaensis* (vs. orange-reddish), *M. chrysochaetes* (vs. golden brown), *M. eleryi* (vs. coppery brown), *M. feae* (vs. dark grayish), *M. jaintiana* (vs. medium gray with brownish tinge), *M. jinchui* (vs. brownish gray), *M. liboensis* (vs. yellowish brown), *M. lorelieae* (vs. reddish brown), *M. walstoni* (vs. brownish gray), *M. walstoni* (vs. warm brown, whitish at the base, orangish brown at tips), and *M. yuanyang* (vs. bark gold). By ventral fur is grayish brown overall (bicolored, dark at the base, pale at tips), *M. milinensis* sp. nov. can be further distinguished from *M. bicolor* (vs. uniformly yellow), *M. rongjiangensis* (vs. bright yellowish orange), and *M. shuipuensis* (vs. bright orange yellow).

By the ears without smooth convex anterior margins and no notch on posterior margin, *Murina yadongensis* sp. nov. can be distinguished from *M. gracilis*, *M. harpioloides*, and *M. kontumensis* (vs. with smoothly convex anterior margins and distinct notch on posterior margin). By the lambdoid crest absent, I^2 almost equal to I^3 in height, C^1 taller than P^4, C_1 equal to P_4 in height and crown area, and *Murina yadongensis* sp. nov. can be further distinguished from *M. gracilis* (vs. lambdoid crest very weak), *M. harpioloides* (vs. I^2 lower than I^3 in height, C^1 less than P^4 in height, and C^1 taller than P^4), and *M. kontumensis* (vs. lambdoid crest present, and C_1 larger than P_4 in height and crown area).

Habitat and ecology. The type locality experiences a subtropical semi-humid monsoon climate, characterized by mild and humid conditions. The average temperature in July is approximately 14.4 °C, and the mean annual precipitation is about 800 mm. The perennial influence of the monsoon, along with the mild and humid climate, contributes to the richness of forest resources in the southern part of the county. The specimen was captured in a harp trap on 6 August 2023 in a mixed coniferous forest in Xiayadong Township, Yadong County. The area is surrounded by dense thickets and bamboo forests, with rivers and primary forests situated approximately 3 kilometers away. In this forest, we also collected five species from four genera: *Plecotus homochrous*, *Rhinolophus sinicus*, *Rhinolophus ferrumequinum*, *Myotis* sp., and *Submyotodon moupinensis*.

Murina rubella Thomas, 1914

Figs 15–17, Table 5, Suppl. material 2

Chresonymy. *Murina huttoni rubella*: Zhang 1997 (Guangxi and Fujian, China); Wang 2003 (Fujian, Jiangxi, and Guangxi, China); Csorba et al. 2007 (China); Francis and Eger 2012 (Fokien, China); Jiang 2015, 2021 (Fujian, Jiangxi, and Guangxi, China); Zhang et al. 2016 (Jinggangshan National Natural Reserve, Jiangxi, China); Moratelli et al. 2019 (Hunan, Jiangxi, Fujian, Guangdong, and Guangxi, China; Myanmar, Thailand, Laos, Vietnam, Peninsular Malaysia). *Murina huttoni*: Zhou et al. 2011 (Guangdong, China); Jiang 2015, 2021 (Fujian, Jiangxi, and Guangxi, China); Huang et al. 2018 (Huibei, Zhejiang, China); Wei 2022 (Xizang, Hubei, Fujian, Jiangxi, Zhejiang, Guangdong, Guangxi, China); Wei et al. 2022 (China); Qin et al. 2023 (Anhui, China); and Liao et al. 2023 (Hunan, China).

Holotype. BMNH 1908.8.11.6., adult male.

Type locality. Kuatun, Fokien, China (Kuatun, Wuyishan City, Fujian Province, China).

Measurements (in mm) holotype. FL: 37.50, GTL: 18.2 (Thomas 1914).

Material examined. • Four male specimens (XZ202387, XZ202399, XZ2023102, and XZ2023104) and three female specimens (XZ2024041, XZ2023101, and XZ2023103) were collected from Xiachayu Town, Zayu County, Nyingchi City, Xizang Autonomous

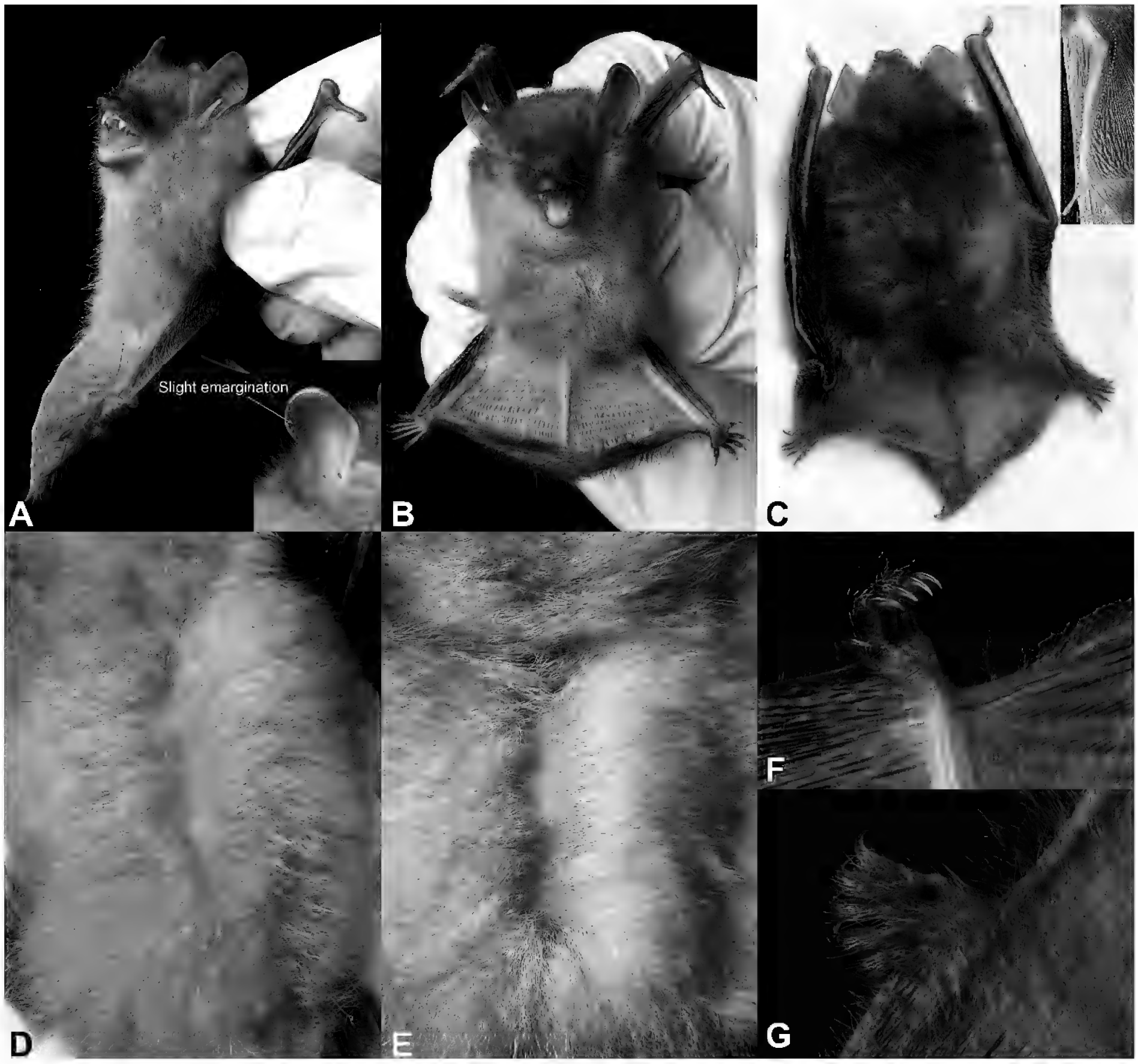

Figure 15. External morphological characteristics of the *M. rubella* in living specimen, GS2024031. **A.** Lateral view; **B.** Ventral view; **C.** Dorsal view of the body and uropatagium; **D.** Ventral hairs; **E.** Dorsal hairs; **F.** Hindfoot ventral view; **G.** Hindfoot dorsal view.

Region, China. • One female specimen (GS20240031, Figu.15) was collected from Yaodu Town, Wen County, Longnan City, Gansu Province, China.

Etymology. The specific epithet "*rubella*" comes from the Latin word *rubellus*, meaning "slightly reddish" or "reddish". The common English name "Fujian Tube-nosed Bat" and the Chinese name "Fú Jiàn Guǎn Bí Fú (福建管鼻蝠)".

Diagnosis. *Murina rubella* can be distinguished from all of the other congeners by the following combination of characters: (1) larger body size, FL 34.24–38.45 mm, GTL 17.08–18.51 mm; (2) dorsal fur tan overall, pale brown at the base, gradually transitioning to dark tan tips from 2/3 from base; (3) ventral fur uniformly pale brown overall, black at the base, gray-white at tips; (4) ears narrow and oval, with smoothly convex anterior margins, no notch on posterior margins; (5) forearm and wrists covered with sparse hairs; (6) wing attachment point located at 1/3 from base of claw to base of toe; (7) without off-white circumferential band around the neck; (8) sagittal and lambdoid crests absent; (9) I^2 is situated anterior to I^3 and clearly visible in lateral view, I^2 slightly smaller than I^3 in height; (10) mesostyles of M^1 and M^2 are slightly reduced; (11) C^1 slightly smaller than P^4 in height, crown is about 2/3 of P^4; (12) P_2 approximately half of P_4 in height, crown area 2/3 that of P^4; (13) C_1 equal to P_4 in height and crown area.

Redescription. Morphometric data of *M. rubella* are provided in Table 5 and Suppl. material 2. Medium-size *Murina*, HB 37.29–48.73 mm, FL 34.24–38.45 mm, EL 16.15–17.68 mm, HFL 7.58–9.49 mm, and BW 4.00–21.00 g. Nostrils tubular, open sideways, and short. Ears slightly large, short, and broadly rounded, blunt at tips, with smoothly convex anterior margins, not notched on posterior margin. Tragus short, narrow, and tapering toward pointed tip, with slightly convex anterior margin, concave posterior margin, and basal notch, and it curves outwards slightly, about half as long as ear. Body covered with thick and fluffy hair. Dorsal hairs tan, similar to rust color (pale brown at the base, gradually transitioning to dark tan tips from 2/3 from

Figure 16. Skull and dentition of the *M. rubella*. **A.** Lateral view; **B.** Dorsal view; **C.** Ventral view; **D.** Frontal view of mandible.

base). Dorsal hairs extend onto bases of wings, uropatagium, thumbs, forearm, and feet, with slight-developed fringe of hairs around margin of uropatagium. Densely furred anterior 1/3 of the dorsal uropatagium, posterior 2/3 covered with sparse hairs. Ventral hairs uniformly pale brown overall. Without off-white circumferential band around the neck. Dark reddish-brown around the eyes, muzzle, and lower forehead, and the face is hairy except for the long, protuberant nostrils that are naked. TL 36.53–40.69 mm, slightly shorter than head-body length, tip of the tail extending significantly past the rear edge of the uropatagium, tip slight free. Plagiopatagium attachment point located at 1/3 from base of claw to base of toe, near base of claw (Fig. 15G).

Skull robust, nearly oval, relatively small, GTL 17.08–18.51 mm. Rostrum long, deep, gradually ascending to forehead; prominent median depression present. Sagittal and lambdoid crests absent. In dorsal view, braincase domed; zygomatic arches weak and slender, gradually widening posteriorly, widest at the base of the zygomatic arches; posterior margin of skull slightly protruding; middle from snout to frontal region distinctly concave downward. In lateral view, skull slightly elongated, with elongated oval braincase; height gradually rising from snout to parietal, with slightly increasing slope from snout to frontal and decreasing slope from frontal to parietal; slight depression between snout and frontal, with distinct prominence at frontal; zygomatic arches gradually rising from anterior to posterior. In ventral view, palatine wide and nearly flat, ending at posterior margin of C^1; basisphenoid pits slightly shallowly teardrop-shaped, extending posteriorly to anterior half of cochlea. Mandible length 11.03–12.49 mm, inverted L-shaped in lateral view. Line between coronoid process and condyle nearly flat; distinct inward depression between condyle and angle; angle short and wide; mandibular foramina clearly visible, situated below anterior margin of P_2.

Dental morphology: Dental formula is I2/3, C1/1, P2/2, M3/3=34 (Fig. 16). In the maxilla, I^2 is situated anterior to I^3, and I^2 clearly visible laterally; crown area of P^2 approximately half that of P^4 and slightly smaller than C^1. Based on these characters, the *M. rubella* belongs to the "*suilla*-type". Maxillary dentition converges slightly anteriorly (RCM = 0.63–0.80). I^2 and I^3 bicuspid, smaller secondary cusp situated posterior to primary cusp; I^2 slightly smaller than I^3 in height, crown area of I^2 2/3 that of I^3; distinct gap between posterior surface of I^3 and C^1, not in contact, about half of height of C^1. C^1 slightly smaller than P^4 in height, slightly elongated and lacking secondary cusps, crown area 2/3 that of P^4. P^2 smaller, delicate and pointed, about half of P^4 and 2/3 of C^1 in height, and crown area of P^2 is half that of P^4 and slightly smaller than C^1. Mesostyles of M^1 and M^2 are reduced, but retaining distinct cusps; paracone, protocone, metacone, and parastyle well developed. M^3 reduced, with only parastyle, paracone, and protocone. In the mandible, I_1, I_2, and I_3 smaller, tricuspid, almost equal in height and width; slight overlap of outer cusps of I_1, I_2, and I_3; with gradual increase in height from I_1 to C_1. C_1 without pointed cusp on anterior inner margin, in contact with I_3 outer

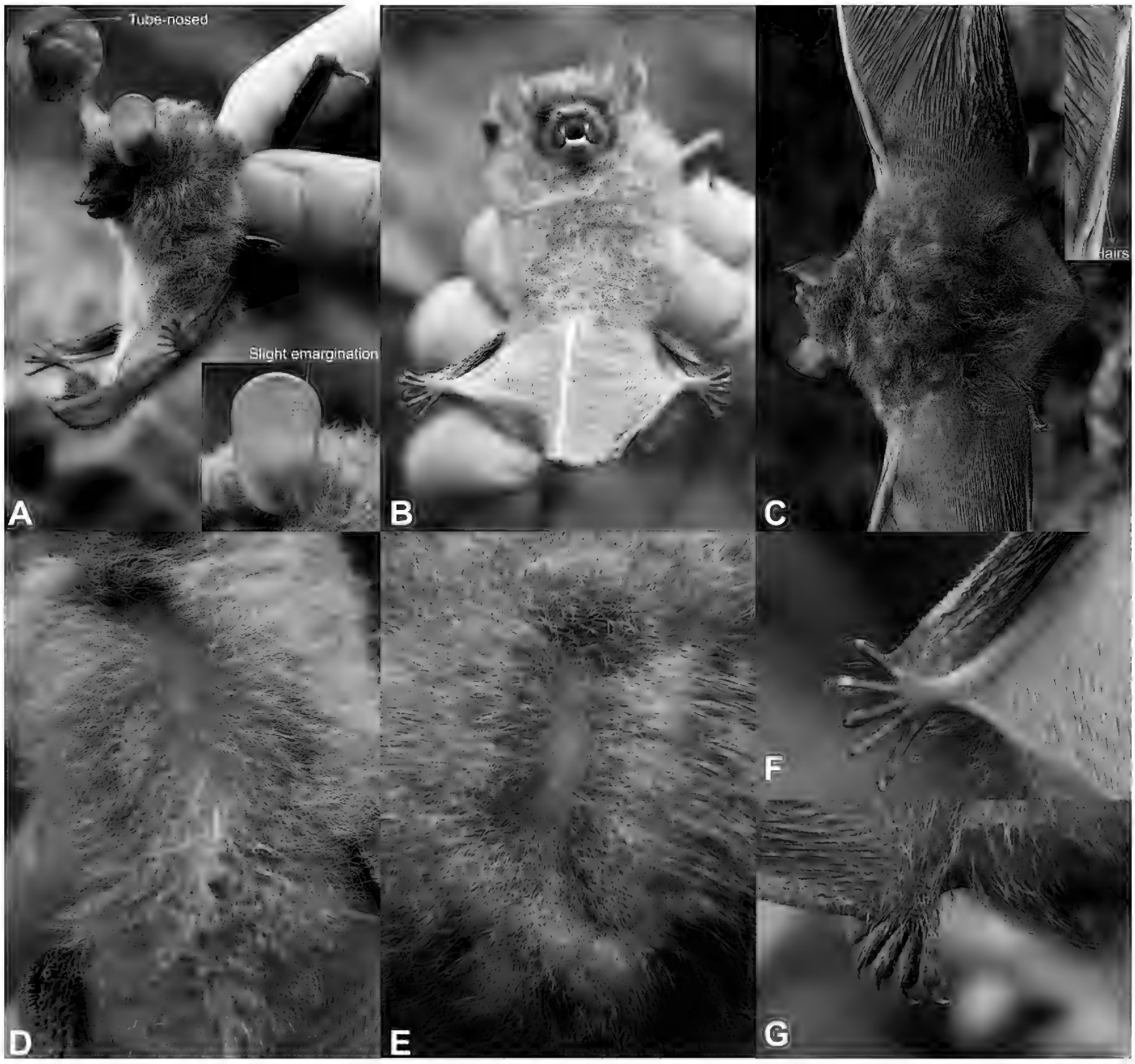

Figure 17. External morphological characteristics of the *M. rubella* in living specimen, XZ2024041. **A.** Lateral view; **B.** Ventral view; **C.** Dorsal view of the body and uropatagium; **D.** Ventral hairs; **E.** Dorsal hairs; **F.** Hindfoot ventral view; **G.** Hindfoot dorsal view.

cusp. C_1 taller than P_4 and equal in basal area to P_4. P_2 exceeded four-fifths of P_4 in height, and the basal and crown areas are about 2/3 of P_4. In lateral view, trigonids of M_1, M_2, and M_3, metaconidhe slightly equal to protoconid in height, paraconid about 1/3 of protoconid. Talonid of M_1 and M_2 almost the same size as trigonid; entoconid and hypoconid distinctly separated from trigonid, lower than metaconid and paraconid, nearly equal to metaconid and paraconid in height. M_1 and M_2 are nyctalodont types, with well-developed entoconids. M_3 reduced, talonid approximately 1/3 as long as trigonid, paraconid, protoconid, and metaconid complete and well developed.

Morphological comparisons with congeneric species. Based on its dentition, I^2 is situated anterior to I^3 and crown area of P^2 approximately half that of P^4 and slightly smaller than C^1, *M. rubella* belongs to the "*suilla*-type", a character that distinguishes 14 species belonging to the "*cyclotis*-type", including *M. aenea*, *M. annamitica*, *M. cyclotis*, *M. fionae*, *M. guilleni*, *M. harrisoni*, *M. huttoni*, *M. peninsularis*, *M. pluvialis*, *M. puta*, *M. recondita*, and *M. rozendaali*. Detailed morphological differences between the *M. rubella* and congeners are shown in Suppl. material 5 and Suppl. material 1: fig. S3.

Murina rubella can be distinguished from *M. beibengensis* sp. nov. by the dorsal hairs dark tan (vs. orangish-yellow overall), from *M. medogensis* sp. nov. (vs. dark grayish), from *M. yadongensis* sp. nov. (vs. brown-gold), *M. milinensis* sp. nov. (vs. brown-gold), from *M. aurata* (vs. golden brown with golden tips), from *M. balaensis* (vs. golden orangish brown, with orange reddish brown tips), from *M. harpioloides* (vs. orangish brown with orange gold tips), from *M. hilgendorfi* (vs. silvery brownish gray), from *M. jaintiana* (vs. medium gray with brownish tinge), from *M. jinchui* (vs. brownish gray), from *M. liboensis* (vs. yellowish brown), from *M. shuipuensis* (vs. golden grayish brown), from *M. suilla* (vs. orangish brown), from *M. tubinaris* (vs. light grayish brown), and from *M. yushuensis* (vs. brown-gold).

Table 5. External and craniodental measurements (in mm) of *M. rubella* and a closely related species. NA indicates that the data is not available.

Species	*M. rubella*		*M. huttoni* (Chakravarty et al. 2020)	*M. puta* (Moratelli et al. 2019)
	Male (n = 4)	Female (n = 4)	Range	Range
BW	4.00–21.00 (12.25 ± 9.54)	6.00–19.00 (10.10 ± 6.08)	8–11	5.4–9.0
HB	37.29–39.26 (38.43 ± 0.82)	42.57–48.73 (44.48 ± 2.88)	NA	59.0–61.0
TL	36.54–40.53 (38.25 ± 1.71)	36.53–40.69 (38.51 ± 1.93)	31.0–37.9	32.0–36.0
EL	16.15–17.68 (17.03 ± 0.66)	16.89–17.51 (17.09 ± 0.29)	14.9–20.9	17.0–19.0
EW	9.09–9.67 (9.33 ± 0.25)	8.14–10.67 (9.51 ± 1.04)	NA	NA
TRL	8.66–9.96 (9.08 ± 0.61)	6.80–9.76 (8.22 ± 1.22)	NA	NA
TRW	2.40–2.61 (2.49 ± 0.09)	1.84–2.63 (2.31 ± 0.35)	NA	NA
HFL	8.27–9.49 (8.83 ± 0.61)	7.58–8.96 (8.47 ± 0.62)	8.0–10.0	10.0–11.0
FL	34.24–36.07 (35.59 ± 0.90)	36.30–38.45 (37.04 ± 1.01)	34.4–36.5	33.0–39.0
TIB	16.98–17.68 (17.37 ± 0.29)	16.55–17.74 (17.28 ± 0.55)	13.0–17.93	NA
GTL	17.08–18.28 (17.61 ± 0.51)	17.13–18.51 (17.82 ± 0.59)	NA	NA
CCL	15.45–16.54 (16.20 ± 0.50)	15.94–17.15 (16.68 ± 0.53)	NA	NA
BCW	7.65–8.07 (7.82 ± 0.20)	7.37–8.21 (7.88 ± 0.37)	NA	NA
BCH	6.94–7.76 (7.44 ± 0.36)	6.70–7.53 (7.19 ± 0.38)	NA	NA
ZYW	9.05–9.76 (9.47 ± 0.35)	9.71–10.20 (9.95 ± 0.25)	NA	NA
MAW	7.64–8.54 (8.02 ± 0.42)	8.21–8.66 (8.37 ± 0.20)	NA	NA
IOW	4.40–4.61 (4.52 ± 0.10)	4.56–4.99 (4.68 ± 0.21)	NA	NA
CM^3L	5.68–6.03 (5.91 ± 0.17)	4.02–6.12 (5.46 ± 0.97)	NA	NA
C^1C^1W	2.81–2.98 (2.87 ± 0.08)	2.93–4.19 (3.55 ± 0.62)	NA	NA
M^3M^3W	3.73–4.47 (4.03 ± 0.32)	4.23–6.02 (5.13 ± 0.95)	NA	NA
RCM	0.63–0.80 (0.72 ± 0.07)	0.66–0.74 (0.69 ± 0.04)	NA	NA
CM_3L	6.61–7.12 (6.83 ± 0.21)	4.63–6.99 (6.17 ± 1.05)	NA	NA
ML	11.03–12.49 (11.46 ± 0.69)	11.43–12.40 (11.85 ± 0.45)	NA	NA
MDL	11.53–14.42 (12.29 ± 1.42)	11.93–12.90 (12.44 ± 0.42)	NA	NA
CPH	4.17–4.61 (4.39 ± 0.18)	4.14–4.64 (4.45 ± 0.22)	NA	NA

Murina rubella can be distinguished from *M. chrysochaetes*, *M. gracilis*, *M. kontumensis*, and *M. yuanyang* by without off-white circumferential band around the neck (vs. absent). By the ears with smooth convex anterior margins, but without notch on posterior margin, *M. rubella* can be distinguished from *M. beelzebub*, *M. bicolor*, *M. eleryi*, *M. fanjingshanensis*, *M. hkakaboraziensis*, *M. leucogaster*, and *M. rongjiangensis* (vs. with distinct notch on posterior margin).

By I^2 less than I^3 in height, *M. rubella* can be distinguished from *M. lorelieae* (vs. I^2 higher than I^3), *M. ryukyuana* (vs. I^2 equal to I^3), and *M. florium* (vs. I^2 higher than I^3). *Murina rubella* different from *M. walstoni* by sagittal and lambdoid crests absent (vs. present) and ventral hairs uniformly pale brown (vs. pure white); from *M. tenebrosa* and *M. florium* by ventral hairs uniformly pale brown (vs. paler).

Habitat and ecology. Specimen GS2023031 was captured on 23 April 2024, using a harp trap in a mixed coniferous and broadleaf forest located at the border between Longnan City, Gansu Province, and Guangyuan City, Sichuan Province, China. The area, situated in the western part of the Qinling Mountains, is surrounded by small-scale agricultural land and tea plantations. Rich in forest resources, the region has a subtropical, mild, and humid climate, with a multi-year average temperature of 16.5 °C and an average annual precipitation of approximately 600 mm. Only one specimen was captured during the survey, and no other bats were observed or captured in subsequent surveys. We speculate that the bats in this area may have been in a post-hibernation stage and were not yet active.

Remark. *Murina rubella* was described on the basis of specimens from the Guadun, Fujian, China, as a subspecies of *M. huttoni* and is widely accepted (Moratelli et al. 2019). Subsequently, *M. huttoni* has been widely recorded from southern provinces of China, including Xizang, Hubei, Fujian, Jiangxi, Zhejiang, Guangdong, Guangxi, Hunan, and Anhui (Zhang 1997; Wang 2003; Zhou et al. 2011; Jiang 2015; Huang et al. 2018; Jiang 2021; Liao et al. 2023; Qin et al. 2023; Wei et al. 2025). Recently, mitochondrial markers of the near-type locality of *M. h. rubella* and *M. huttoni* were published (Zhang et al. 2016; Chakravarty et al. 2020), offering the possibility of resolving the phylogenetic relationships of these two species. In our phylogenetic tree reconstructed on the basis of mitochondrial COI, the *M. huttoni* complex from different regions formed seven clades: Clade i included *M. huttoni* from the near type locality; Clade ii included the species *M. puta*; Clade iii was from central Vietnam; and Clade iv was from southern China (Guangdong, Hunan, Jiangxi), including the near-type locality *M. rubella*; Clades v and vi are from Xizang, China; and Clade vii is from China (Hunan), Vietnam, and central Laos. From the results of the mPTP species delimitation, Clades i, ii, and iii-vii are proposed as separate species, with genet-

ic distances between them ranging from 6.2% to 6.9%. Based on this evidence, and the validity of *M. huttoni* and *M. puta* is recognized, then the proposal to elevate the subspecies *M. h. rubella* in China to species status should be accepted. For *M. huttoni*, we speculate that its distribution in China may be limited to the territory of Xizang Autonomous Region, along the Himalaya.

Geographic distribution. Based on this study, phylogenetic evidence, and previous literature, *M. rubella* can be definitively recorded as distributed in China (Anhui, Fujian, Guangxi, Guangdong, Hubei, Hunan, Jiangxi, Zhejiang, Xizang) (Zhang 1997; Wang 2003; Francis et al. 2010; Zhou et al. 2011; Jiang 2015; Zhang et al. 2016; Huang et al. 2018; Moratelli et al. 2019; Yu et al. 2020; Jiang 2021; Liao et al. 2023; Qin et al. 2023), northern Laos (Francis et al. 2010; Francis and Eger 2012; Nguyen et al. 2015b), and Vietnam (Francis and Eger 2012; Tu et al. 2015; Tu et al. 2016). Although *M. huttoni* has also been recorded in northern Thailand, northern Myanmar, and Peninsular Malaysia (Moratelli et al. 2019), the authenticity of these records (Francis and Eger 2012) requires further evidence due to the lack of available genetic data. The *M. huttoni sensu stricto* may be confined to the periphery of the Himalayas (Moratelli et al. 2019).

Discussion

Asian tube-nosed bats, genus *Murina*, are the most frequently described taxon among bats in China in recent years, and seven species have been described, i.e., *M. fanjingshanensis* (He et al. 2015), *M. rongjiangensis* (Chen et al. 2017), *M. liboensis* (Zeng et al. 2018), *M. jinchui* (Yu et al. 2020), *M. yuanyang* (Mou et al. 2024), *M. yushuensis* (Wang et al. 2024a), and *M. lvchun* (Mou et al. 2025). We describe here four new species, named *Murina beibengensis* sp. nov., *Murina medogensis* sp. nov., *Murina milinensis* sp. nov., and *Murina yadongensis* sp. nov., based on fieldwork in Xizang, China, in the last three years, combined with morphological (refer to previous species descriptions), mitochondrial COI, and Cyt *b*. Morphologically, these four new species can be distinguished from conspecifics based on differences in body fur color, forearm length, dentition, and skull (Suppl. material 1: table S9). In the phylogeny, the four new species formed distinct lineages, with mitochondrial COI and Cyt *b* divergences from congeners ranging from 7.0% to 20.3% and 6.1% to 17.2%, respectively. These divergences are significantly greater than those observed among currently recognized species (Suppl. material 1: tables S3, S4). Thus, morphological and genetic evidence supports the validity of these four new species. The discovery of these four new species indicates that the diversity of the genus *Murina* is significantly underestimated, particularly in the Himalayan and Qinghai-Tibetan Plateau regions. This finding underscores the importance and urgency of conducting comprehensive surveys in these areas.

Due to the sampling constraints in evergreen broadleaved forests where only harp traps can be effectively deployed, we obtained only one to two specimens each of *Murina beibengensis* sp. nov. and *Murina medogensis* sp. nov. Despite the limited sample size, multiple lines of evidence support their validity as distinct species. Similar situations with small type series, e.g., *M. lvchun* with two specimens (Mou et al. 2025), *M. yushuensis* with one specimen (Wang et al. 2024a), and *M. hkakaboraziensis* with one specimen (Soisook et al. 2017), are not uncommon in chiropteran taxonomy, particularly for rare forest-dwelling species. While we acknowledge that future collections may expand the known morphological variation ranges, the current diagnostic characters, including both discrete morphological features and genetic divergence, provide robust support for their taxonomic recognition. The congruence between morphological distinctiveness and genetic differentiation observed in our analyses strongly suggests these represent valid species rather than intraspecific variants.

Most species of the genus *Murina* have been found in montane forests at elevations ranging from 110 m to 2600 m (Moratelli et al. 2019) with the exception of *M. yushuensis* (3770 m) (Wang et al. 2024a). The four new species described here are distributed across low to mid-altitude regions of the Himalayas, though they may also inhabit higher elevations. For example, *Murina beibengensis* sp. nov. has been recorded at elevations ranging from 864 m to 4414 m. This remarkable altitudinal variation suggests that *Murina beibengensis* sp. nov. exhibits strong locomotor capabilities and may possess unique adaptations to cope with rapid environmental changes during flight, such as high temperatures and low oxygen levels. Future genomic studies of this species will provide valuable insights into the genetic mechanisms underlying its adaptation to high-altitude environments. This study describes four new species of *Murina* and elevates the subspecies *M. huttoni rubella* to species rank, increasing the total number of recognized species in the genus from 43 to 48. Given the low dispersal capability and relatively small natural population densities characteristic of *Murina* bats, additional conservation measures are warranted to ensure their long-term survival.

Acknowledgments

This study was supported by the program of the Survey of Wildlife Resources in Key Areas of Tibet (Phase II), Survey of Wildlife Resources in Key Areas of Tibet (ZL202203601), and Diversity and Distribution Survey of Chiroptera species in China (2021FY100302). We thank Xin-Rui Zhao, Peng-Fei Luo, Qing-Qing He, and Qin Yang for their help during the sample collection. We thank Dr. Jing-Song Shi for his help with the CT scan of the bones.

References

Bhattacharyya T (2002) Taxonomic status of the genus *Harpiola* Thomas, 1915 (Mammalia, Chiroptera, Vespertilionidae), with a report of the occurrence of *Harpiola grisea* (Peters, 1872) in Mizoram, India. Proceedings of the Zoological Society, Calcutta 55(1): 73–76.

Blair C, Bryson Jr RW (2017) Cryptic diversity and discordance in single-locus species delimitation methods within horned lizards (Phrynosomatidae, *Phrynosoma*). Molecular Ecology Resources 17(6): 1168–1182. https://doi.org/10.1111/1755-0998.12658

Chakravarty R, Ruedi M, Ishtiaq F (2020) A recent survey of bats with descriptions of echolocation calls and new records from the western Himalayan region of Uttarakhand, India. Acta Chiropterologica 22(1): 197–224. https://doi.org/10.3161/15081109ACC2020.22.1.019

Chen J, Liu T, Deng HQ, Xiao N, Zhou J (2017) A new species of *Murina* bats was discovered in Guizhou Province, China. Cave Research 2(1): 1–10.

Corbet GB, Hill JE (1992) The mammals of the Indomalayan region: a systematic review. Oxford University Press, Oxford, 488 pp.

Csorba G, Bates PJJ (2005) Description of a new species of *Murina* from Cambodia (Chiroptera, Vespertilionidae, Murininae). Acta Chiropterologica 7(1): 1–7. https://doi.org/10.3161/1733-5329(2005)7[1:DOANSO]2.0.CO;2

Csorba G, Thong VD, Bates PJ, Furey NM (2007) Description of a new species of *Murina* from Vietnam (Chiroptera: Vespertilionidae: Murininae). Occasional Papers, Museum of Texas Tech University 268: 1–12. https://doi.org/10.5962/bhl.title.156958

Csorba G, Son NT, Saveng I, Furey NM (2011) Revealing cryptic bat diversity: three new *Murina* and redescription of *M. tubinaris* from Southeast Asia. Journal of Mammalogy 92(4): 891–904. https://doi.org/10.1644/10-MAMM-A-269.1

Dobson G (1872) Notes on some bats collected by Captain WG Murray, in the North-Western Himalaya, with description of new species. In: Proceedings of the Asiatic Society of Bengal, 208–210.

Edgar RC (2004) MUSCLE: multiple sequence alignment with high accuracy and high throughput. Nucleic Acids Research 32(5): 1792–1797. https://doi.org/10.1093/nar/gkh340

Eger JL, Lim BK (2011) Three new species of *Murina* from southern China (Chiroptera, Vespertilionidae). Acta Chiropterologica 13(2): 227–243. https://doi.org/10.3161/150811011X624730

Francis CM, Eger JL (2012) A review of tube-nosed bats (*Murina*) from Laos with a description of two new species. Acta Chiropterologica 14(1): 15–38. https://doi.org/10.3161/150811012X654231

Francis CM, Borisenko AV, Ivanova NV, Eger JL, Lim BK, Guillén-Servent A, Kruskop SV, Mackie I, Hebert PDN (2010) The Role of DNA Barcodes in Understanding and Conservation of Mammal Diversity in Southeast Asia. PLoS ONE 5(9): e12575. https://doi.org/10.1371/journal.pone.0012575

Furey NM, Thong VD, Bates PJ, Csorba G (2009) Description of a new species belonging to the *Murina* '*suilla*-group' (Chiroptera, Vespertilionidae, Murininae) from North Vietnam. Acta Chiropterologica 11(2): 225–236. https://doi.org/10.3161/150811009X485477

He F, Xiao N, Zhou J (2015) A new species of *Murina* from China (Chiroptera, Vespertilionidae). Cave Research 2(2): 2–6.

Hill J (1964) Notes on some tube-nosed bats, genus *Murina*, from southeastern Asia, with descriptions of a new species and a new subspecies. Federation Museums Journal 8: 48–59.

Hill J, Francis CM (1984) New bats (Mammalia: Chiroptera) and new records of bats from Borneo and Malaya. 47(5): 305–329. https://doi.org/10.5962/p.21841

Hoang DT, Chernomor O, Von Haeseler A, Minh BQ, Vinh LS (2018) UFBoot2: improving the ultrafast bootstrap approximation. Molecular Biology and Evolution 35(2): 518–522. https://doi.org/10.1093/molbev/msx281

Huang ZL, Hu Y, Wu H, Cao Y, Liu B, Zhou J, Wu Y, Yu W (2018) New Distribution Record of *Murina huttoni* in Hubei and Zhejiang Provinces. Journal of West China Forestry Science 47(6): https://doi.org/10.16473/j.cnki.xblykx1972.2018.06.013

Jiang Z (2015) China's Mammal Diversity and Geographic Distribution. Science Press, Beijing, 133 pp.

Jiang Z (2021) China's Red List of Biodiversity: Vertebrates Volume l, Mammals (l). Science Press, Beijing, 892–893.

Kapli P, Lutteropp S, Zhang J, Kobert K, Pavlidis P, Stamatakis A, Flouri T (2017) Multi-rate Poisson tree processes for single-locus species delimitation under maximum likelihood and Markov chain Monte Carlo. Bioinformatics 33(11): 1630–1638. https://doi.org/10.1093/bioinformatics/btx025

Kruskop SV, Eger JL (2008) A new species of tube-nosed bat *Murina* (Vespertilionidae, Chiroptera) from Vietnam. Acta Chiropterologica 10(2): 213–220. https://doi.org/10.3161/150811008X414809

Kumar S, Stecher G, Tamura K (2016) MEGA7: molecular evolutionary genetics analysis version 7.0 for bigger datasets. Molecular Biology and Evolution 33(7): 1870–1874. https://doi.org/10.1093/molbev/msw054

Kuo HC, Fang YP, Csorba G, Lee LL (2006) The definition of *Harpiola* (Vespertilionidae, Murininae) and the description of a new species from Taiwan. Acta Chiropterologica 8(1): 11–19. https://doi.org/10.3161/1733-5329(2006)8[11:TDOHVM]2.0.CO;2

Kuo HC, Fang YP, Csorba G, Lee LL (2009) Three New Species of *Murina* (Chiroptera, Vespertilionidae) from Taiwan. Journal of Mammalogy 90(4): 980–991. https://doi.org/10.1644/08-MAMM-A-036.1

Lanfear R, Frandsen PB, Wright AM, Senfeld T, Calcott B (2017) PartitionFinder 2: new methods for selecting partitioned models of evolution for molecular and morphological phylogenetic analyses. Molecular Biology and Evolution 34(3): 772–773. https://doi.org/10.1093/molbev/msw260

Liao YQ, Huang ZF, Xie HX, Liang XL, He MY, Deng WP, Wu Y, Wang XY, Yu WH (2023) *Myotis rufoniger* and *Murina huttoni* Found in Hunan, China. Chinese Journal of Zoology 58(8): 772–779. https://doi.org/10.13859/j.cjz.202305011

Maeda K, Matsumura S (1998) Two New Species of Vespertilionid Bats, *Myotis* and *Murina* (Vespertilionidae, Chiroptera) from Yanbaru, Okinawa Island, Okinawa Prefecture, Japan. Zoological Science 15(2): 301–307. https://doi.org/10.2108/zsj.15.301

Moratelli R, Burgin C, Cláudio V, Novaes R, López-Baucells A, Haslauert R (2019) Family Vespertilionidae (Vesper Bats). In: Wilson DE, Mittermeier RA (Eds) Handbook of the Mammals of the World-Vol 9, Bats. Lynx Edicions, Barcelona (Spain), 855–996.

Mou X, Qian Y, Li M, Li B, Luo X, Li S (2024) A New Species of *Murina* (Chiroptera, Vespertilionidae) from Yunnan, China. Animals 14(16): 2371. https://doi.org/10.3390/ani14162371

Mou X, Qian Y, Wang W, Zhang W, Wang J, Li S (2025) A New '*cyclotis*-morphotype' Species of Tube-Nosed Bat (Chiroptera, Vespertilionidae, *Murina*) from China. Animals 15(1): 75. https://doi.org/10.3390/ani15010075

Nguyen LT, Schmidt HA, Von Haeseler A, Minh BQ (2015a) IQ-TREE: a fast and effective stochastic algorithm for estimating maximum-likelihood phylogenies. Molecular Biology and Evolution 32(1): 268–274. https://doi.org/10.1093/molbev/msu300

Nguyen TS, Masaharu M, Tatsuo O, Vu Dinh T, Gabor C, Hideki E (2015b) Multivariate Analysis of the Skull Size and Shape in Tube-Nosed Bats of the Genus *Murina* (Chiroptera, Vespertilionidae) from Vietnam. Mammal Study 40(2): 79–94. https://doi.org/10.3106/041.040.0203

Peters W (1872) Mittheilung über neue Flederthiere. Monatsberichteder Königlich Preussischen Akademie der Wissenschaften zu Berlin 1872: 256–264.

Qin B, Zhu H, Liao Y, Chen Z, Wang X, Zhang Y, Chu J, Yu W, Wu Y (2023) A New Record of *Murina huttoni* (Chiroptera, Vespertilionidae) from Anhui Province, China. Sichuan Journal of Zoology 42(6): 688–694. https://doi.org/10.11984/j.issn.1000-7083.20230098

Ronquist F, Teslenko M, Van Der Mark P, Ayres DL, Darling A, Höhna S, Larget B, Liu L, Suchard MA, Huelsenbeck JP (2012) MrBayes 3.2: efficient Bayesian phylogenetic inference and model choice across a large model space. Systematic Biology 61(3): 539–542. https://doi.org/10.1093/sysbio/sys029

Ruedi M, Biswas J, Csorba G (2012) Bats from the wet: two new species of Tube-nosed bats (Chiroptera, Vespertilionidae) from Meghalaya, India. Revue Suisse de Zoologie 119(1): 111–135. https://doi.org/10.5962/bhl.part.150145

Scully J (1881) On the mammals of Gilgit. In: Proceedings of the Zoological Society of London. Wiley Online Library, 197–209. https://doi.org/10.1111/j.1096-3642.1881.tb01278.x

Soisook P (2013) Systematics, Biogeography and Echolocation of Tube-nosed Bats Genus *Murina* (Chiroptera, Vespertilionidae) in Mainland Southeast Asia. Songkhla: Prince of Songkla University, 1–181.

Soisook P, Karapan S, Satasook C, Thong VD, Khan FAA, Maryanto I, Csorba G, Furey N, Aul B, Bates PJ (2013a) A review of the *Murina cyclotis* complex (Chiroptera, Vespertilionidae) with descriptions of a new species and subspecies. Acta Chiropterologica 15(2): 271–292. https://doi.org/10.3161/150811013X678928

Soisook P, Karapan S, Satasook C, Bates PJ (2013b) A new species of *Murina* (Mammalia, Chiroptera, Vespertilionidae) from peninsular Thailand. Zootaxa 3746(4): 567–579. https://doi.org/10.11646/zootaxa.3746.4.4

Soisook P, Thaw WN, Kyaw M, Oo SSL, Pimsai A, Suarez-Rubio M, Renner SC (2017) A new species of *Murina* (Chiroptera, Vespertilionidae) from sub-Himalayan forests of northern Myanmar. Zootaxa 4320(1): 159–172. https://doi.org/10.11646/zootaxa.4320.1.9

Son NT, Csorba G, Tu VT, Thong VD, Wu Y, Harada M, Oshida T, Endo H, Motokawa M (2015) A new species of the genus *Murina* (Chiroptera, Vespertilionidae) from the Central Highlands of Vietnam with a review of the subfamily Murininae in Vietnam. Acta Chiropterologica 17(2): 201–232. https://doi.org/10.3161/15081109ACC2015.17.2.001

Sowerby AdC (1922) On a New Bat from Manchuria. Journal of Mammalogy 3(1): 46–47. https://doi.org/10.2307/1373453

Tate GHH (1941) Results of the Archbold Expeditions. No 40. Notes on vespertilionid bats of the subfamily Miniopterinae, Murininae, Kerivoulinae, and Nyctophilinae. Bulletin of the American Museum of Natural History 78(10): 567–597.

Thomas O (1891) Diagnoses of three new mammals collected by Signor L. Fea in the Carin Hills, Burma. Annali del Museo Civico di Storia Naturale di Genova 30(2,10): 884.

Thomas O (1914) New Asiatic and Australian bats and a new bandicoot. The Annals and Magazine of Natural History, including Zoology, Botany, and Geology 13: 439–444. https://doi.org/10.1080/00222931408693506

Tu VT, Cornette R, Utge J, Hassanin A (2015) First records of *Murina lorelieae* (Chiroptera, Vespertilionidae) from Vietnam. Mammalia 79(2): 201–213. https://doi.org/10.1515/mammalia-2013-0101

Tu VT, Estók P, Csorba G, Son NT, Thanh HT, Tuan LQ, Görföl T (2016) Recent remarkable records reveal that Phia Oac-Phia Den Nature Reserve is a priority area for bat conservation in Northern Vietnam. Journal of Asia-Pacific Biodiversity 9(3): 312–322. https://doi.org/10.1016/j.japb.2016.04.007

Wang YX (2003) A Complete Checklist of Mammal species and Subspecies in China: A Taxonomic and Geographic Reference. China Forestry Publishing House, Beijing, 57–59.

Wang X, Han X, Csorba G, Wu Y, Chen H, Zhao X, Dong Z, Yu W, Lu Z (2024a) A new species of Tube-nosed Bat (Chiroptera, Vespertilionidae, *Murina*) from Qinghai-Tibet Plateau, China. Journal of Mammalogy: gyae104. https://doi.org/10.1093/jmammal/gyae104

Wang X, Liang X, Li Y, Csorba G, Hu Y, He K, Wu Y, Yu W (2024b) Phylogenetic conflict between species tree and mitochondrial gene trees in Murininae (Mammalia, Chiroptera) and validation of the genus *Harpiola*. Zoologica Scripta 54(3): 305–316. https://doi.org/10.1111/zsc.12708

Wei F, Yang QS, Wu Y, Jiang XL, Liu SY, Li B, Yang G, Li M, Zhou J, Li S, Hu Y, Ge D, Li S, Yu W, Chen B, Zhang Z, Zhou C, Wu S, Zhang L, Chen Z, Chen S, Deng H, Jiang T, Zhang L, Shi H, Lu X, Li Q, Liu Z, Cui Y, Li Y (2021) Catalogue of mammals in China (2021). Acta Theriologica Sinica 41(5): 487–501. https://doi.org/10.16829/j.slxb.150595

Wei F, Yang QS, Wu Y, Jiang XL, Liu SY, Hu Y, Ge D, Li B, Yang G, Li M, Zhou J, Li S, Li S, Yu W, Chen B, Zhang Z, Zhou C, Wu S, Zhang L, Chen Z, Chen S, Deng H, Jiang T, Zhang L, Shi H, Lu X, Li Q, Liu Z, Cui Y, Li Y, He K (2025) Catalogue of mammals in China (2024). Acta Theriologica Sinica 45(1): 1–16. https://doi.org/10.16829/j.slxb.151039

Wei FW, Yang QS, Wu Y, Jiang XL, Liu SY (2022) Taxonomy and Distribution of Mammals in China. Science Press, Beijing, 337–338.

Wilson DE, Reeder DM (2005) Mammal species of the world: a taxonomic and geographic reference (3rd edn). Johns Hopkins University Press, Baltimore, 312–529.

Yu WH, Csorba G, Wu Y (2020) Tube-nosed variations-a new species of the genus *Murina* (Chiroptera, Vespertilionidae) from China. Zoological Research 41(1): 70–77. https://doi.org/10.24272/j.issn.2095-8137.2020.009

Zeng X, Chen J, Deng H, Xiao N, Zhou J (2018) A new species of *Murina* from China (Chiroptera, Vespertilionidae). Ekoloji 103(27): 9–16.

Zhang RZ (1997) Distribution of Mammal Species in China. China Forestry Publishing House, Beijing, 53–54.

Zhang Q, Cong H, Yu W, Kong L, Wang Y, Li Y, Wu Y (2016) The mitochondrial genome of *Murina huttoni rubella* (Chiroptera, Vespertilionidae) from China. Mitochondrial DNA Part B Resources 1(1): 438–440. https://doi.org/10.1080/23802359.2016.1180557

Zhou Q, Zhang YJ, Masaharu M, Masashi H, Gong YN, Li YC, Wu Y (2011) A New Record Bat *Murina huttonii* from Guangdong, China and Its Morphology, Karyotypes, Echolocation Calls. Chinese Journal of Zoology 6(1): 109–114. https://doi.org/10.13859/j.cjz.2011.01.017

Supplementary material 1

Additional figures and tables

Authors: Tao Luo, Ming-Le Mao, Chang-Ting Lan, Zi-Fa Zhao, Zhong-Lian Wang, Jing Yu, Jia-Jia Wang, Chen-Rui Yan, Ning Xiao, Jiang Zhou

Data type: pdf

Explanation note: **fig. S1.** For the genus *Murina*, a phylogenetic tree (ML) was reconstructed based on the mitochondrial COI gene. **fig. S2.** For the genus *Murina*, a phylogenetic tree (ML) was reconstructed based on the mitochondrial Cyt *b* gene. **fig. S3.** External morphology and skull features of species of the genus *Murina*, from literature and web pages. **table S2.** For the genus *Murina*, locality, voucher information, and mitochondrial COI GenBank accession numbers are provided for all samples used. **table S3.** For the genus *Murina*, locality, voucher information, and mitochondrial Cyt *b* GenBank accession numbers are provided for all samples used. **table S4.** For the *M. huttoni* complex, locality, voucher information, and mitochondrial COI GenBank accession numbers are provided for all samples used. **table S7.** Uncorrected *p*-distance (%) between species of the *M. huttoni* complex based on mitochondrial COI. **table S8.** Results and percentage of variance explained by principal component analysis for *M. beibengensis* sp. nov. and three closely related species. **table S9.** Results and percentage of variance explained by principal component analysis for *M. medogensis* sp. nov. and three closely related species. **table S10.** Results and percentage of variance explained by principal component analysis for *M. milinensis* sp. nov., *M. yadongensis* sp. nov., and four closely related species.

Link: https://doi.org/10.3897/zse.101.144375.suppl1

Supplementary material 2

Raw measurements of species were measured and collected in this study

Authors: Tao Luo, Ming-Le Mao, Chang-Ting Lan, Zi-Fa Zhao, Zhong-Lian Wang, Jing Yu, Jia-Jia Wang, Chen-Rui Yan, Ning Xiao, Jiang Zhou

Data type: xlsx

Explanation note: For closely related species, mean values were also considered.

Link: https://doi.org/10.3897/zse.101.144375.suppl2

Supplementary material 3

Uncorrected *p*-distance (%) between species of the genus *Murina* based on mitochondrial COI

Authors: Tao Luo, Ming-Le Mao, Chang-Ting Lan, Zi-Fa Zhao, Zhong-Lian Wang, Jing Yu, Jia-Jia Wang, Chen-Rui Yan, Ning Xiao, Jiang Zhou

Data type: xlsx

Link: https://doi.org/10.3897/zse.101.144375.suppl3

Supplementary material 4

Uncorrected *p*-distance (%) between species of the genus *Murina* based on mitochondrial Cyt *b*

Authors: Tao Luo, Ming-Le Mao, Chang-Ting Lan, Zi-Fa Zhao, Zhong-Lian Wang, Jing Yu, Jia-Jia Wang, Chen-Rui Yan, Ning Xiao, Jiang Zhou

Data type: xlsx

Link: https://doi.org/10.3897/zse.101.144375.suppl4

Supplementary material 5

Comparison of the diagnostic features of the four new species described here with those selected for the 43 recognized species of the genus *Murina*

Authors: Tao Luo, Ming-Le Mao, Chang-Ting Lan, Zi-Fa Zhao, Zhong-Lian Wang, Jing Yu, Jia-Jia Wang, Chen-Rui Yan, Ning Xiao, Jiang Zhou

Data type: xlsx

Link: https://doi.org/10.3897/zse.101.144375.suppl5